UNIVERSITATEA BABEŞ-BOLYAI
Facultatea de Chimie și Inginerie Chimică

UNIVERSITÄT LEIPZIG
Fakultät für Chemie und Mineralogie

Summary of the Ph. D. Thesis

Novel ferrocenyl- and phenothiazinyl-phosphine ligands: syntheses, transition metal complexes and applications

Scientific advisors

Prof. Dr. Luminița Silaghi-Dumitrescu
Prof. Dr. Evamarie Hey-Hawkins

Ph. D. candidate

Iudit-Hajnal Filip

Cluj-Napoca
2014

JURY

PRESIDENT

Prof. Dr. Liana Mureșan – Facultatea de Chimie și Inginerie Chimică, Universitatea Babeș-Bolyai, Cluj-Napoca

REVIEWERS

CSI Dr. Otilia Costișor - Institutul de Chimie Timișoara al Academiei Române, Timișoara.

Acad. Prof. Dr. Ionel Haiduc - Facultatea de Chimie și Inginerie Chimică, Universitatea Babeș-Bolyai, Cluj-Napoca.

Prof. Dr. Berthold Kersting - Fakultät für Chemie und Mineralogie, Universität Leipzig, Germany

Date of public defence: 19th of September, 2014

Iudit-Hajnal Filip – Ph.D. thesis summary

CONTENTS (as in the full text)

I. General introduction 2

II. Ferrocenyl-phosphine ligands and their transitional metal complexes 4

II.1. Introduction 5

II.2. Literature overview 6

II.2.1. Chirality in ferrocenyl ligands 7

II.2.2. General synthetic routes to asymmetric ferrocenes 10

II.2.2.1. Synthetic routes to 1,1'-asymmetric ferrocenes 11

II.2.2.2. Synthetic routes to 1,2-asymmetric ferrocenes 12

II.2.3. Transition metal complexes of ferrocenylphosphines 18

II.2.4. Conclusions 21

II.3. Original contributions 22

II.3.1. Synthesis of monophosphine $FcCH_2P^t$BuPh (**4**), phosphonium salt $[(FcCH_2)_2P^t\text{BuPh}]^+I^-$ (**5**) and phosphine oxide $FcCH_2P(O)^t$BuPh (**6**) 22

II.3.2. Synthesis of bisphosphines [1-(^{t}BuPhP)CH_2]-2-(^{t}BuPhP)Fc (**9a**) and [1-(^{t}BuPhP)CH(CH_3)]-2-(^{t}BuPhP)Fc (**9b**) and aminophosphine **10** 27

II.3.3. Synthesis of [$PdCl_2${[1-(^{t}BuPhP)CH_2]-2-(^{t}BuPhP)Fc}] (**12a**) and [$PdCl_2${[1-(^{t}BuPhP)CH(CH_3)]-2-(^{t}BuPhP)Fc}] (**12b**) 35

II.3.4. Synthesis of [RhCl{[1-(^{t}BuPhP)CH(CH_3)]-2-(^{t}BuPhP)Fc}]$_2$ (**13**) 39

II.3.5. Conclusions 40

II.4. Experimental part 41

III. Phenothiazinyl-phosphines and their transition metal complexes 51

III.1. Introduction 52

III.2. Literature overview 53

III.2.1. Preparation of bidentate phosphines of heteroarenes and their use in catalysis 53

III.2.2. Preparation of monophosphines of heteroarenes and their use in catalysis 59

III.3. Original contributions 64

III.3.1. Synthesis of phenothiazinyl-phosphites 64

III.3.2. Synthesis of phenothiazinyl-phosphines 66

III.3.3. Transition metal complexes 73

III.3.4. Catalytic activity of phenothiazinyl-phosphines in hydrogenation reactions 83

III.3.5. Biological activity of phenothiazinyl-phosphines and their transition metal complexes 88

III.3.5.1. Interaction with DNA 88
III.3.5.2. Cytotoxicity of complexes **26b** and **27b** 89
III.3.6. Conclusions 91
III.4. Experimental part 92
IV. Palladium complexes of *N*-alkyl-phenothiazines 110
IV.1. Introduction 111
IV.2. Literature overview 112
IV.2.1. Sulfur-metal bonds 112
IV.3. Original contributions 114
IV.3.1. Synthesis and X-ray crystal structure of palladium complexes of *N*-alkyl-phenothiazines 114
IV.3.2. Conclusions 118
IV.4. Experimental section 119
V. Microwave-assisted synthesis and electrochemical characterization of bis-(10*H*-phenothiazin-3-yl)-methane derivatives 124
V.1. Introduction 125
V.2. Original contributions 126
V.2.1. Microwave-assisted synthesis of bis-(10*H*-phenothiazin-3-yl)-methane derivatives 126
V.2.2. Conclusions 133
V.3. Experimental section 134
General conclusions 138
Appendix 1. Abbreviations 139
A 1.1. General abbreviations 139
A 1.2. Abbreviations for groups and substituents 139
A 1.3. Abbreviations for NMR, IR and mass spectra 140
Appendix 2. Crystal data and structural refinement 141
A 2.1. Data for $FcCH_2P^{t}BuPh$ (**4**) 141
A 2.2. Data for $[(FcCH_2)_2P^{t}BuPh]^{+}I^{-}\cdot CH_3OH$ (**5**) 142
A 2.3. Data for $[1\text{-}({}^{t}BuPhP)CH_2]\text{-}2\text{-}({}^{t}BuPhP)Fc$ (**9a**) 143
A 2.4. Data for $[1\text{-}({}^{t}BuPhP)CH(CH_3)]\text{-}2\text{-}({}^{t}BuPhP)Fc$ (**9b**) 144
A 2.5. Data for $[PdCl_2\{[1\text{-}({}^{t}BuPhP)CH_2]\text{-}2\text{-}({}^{t}BuPhP)Fc\}]\cdot 2CH_2Cl_2$ (**12a**) 145
A 2.6. Data for $[PdCl_2\{[1\text{-}({}^{t}BuPhP)CH(CH_3)]\text{-}2\text{-}({}^{t}BuPhP)Fc\}]\cdot 3CH_2Cl_2$ (**12b**) 146
A 2.7. Data for $[PdCl_2\{(10\text{-}Me\text{-}1\text{-}PPh_2\text{-}Ptz)\text{-}\kappa^2 N,P\}]\cdot CH_2Cl_2$ (**25a**) 147
A 2.8. Data for $[PdCl_2\{(10\text{-}Me\text{-}3\text{-}PPh_2\text{-}Ptz)\text{-}\kappa P\}_2]$ (**26a**) 148

A 2.9. Data for [$PdCl_2${(10-Et-4-PPh_2-Ptz)-κ^2*S*,*P*}] (**27a**) 149

A 2.10. Data for [$PtCl_2${(10-Et-4-PPh_2-Ptz)-κ^2*S*,*P*}] (**27b**) 150

A 2.11. Data for [$PdCl_2${(10-Me-Ptz)-κ*S*}$_2$] (**28a**) 151

A 2.12. Data for [$PdCl_2${(10-Et-Ptz)-κ*S*}$_2$] (**28b**) 152

Keywords: ferrocenyl phosphines, phenothiazinyl phosphines, transition metal complexes, cytotoxic activity

I. General introduction

The interest in phosphorus-based compounds of the type PR_3 (where R is an alkyl or aryl group) begun with the first synthesis of trimethylphosphine, by reacting methyl chloride with calcium phosphide at 180-300 °C by Thenard in 1847 [1]. The ability of phosphines to assist the control and selectivity of catalytic transformations is responsible for this interest. Phosphine ligands are excellent soft-donor ligands with a wide variety of easily adjusted steric and electronic factors. Because of the three R-groups and the overall tetrahedral coordination geometry, tertiary phosphines are the most versatile of the neutral 2-electron donor ligands. Variation of the 3 R-groups may induce:

- Changes in the donor/acceptor properties of the phosphines (from excellent donor/poor π-acceptor to poor donor/excellent π-acceptor
- Changes in the steric profile of the phosphine (from small to large molecules)
- Generation of a large number of polydentate polyphosphines (bis-, tris-, tetra-, penta- and hexaphosphine ligands are all known) that can adopt specific coordination geometries.

Phosphines are useful in organometallic and inorganic chemistry largely because the phosphorus possesses a lone pair that enables the phosphine to create new bonds to the phosphorus, such as coordination to transition metals via donation of the lone pair into a vacant metal bonding orbital. This thesis presents the synthesis and structural characterization of phosphine ligands, their transition metal complexes and the use of some of these complexes in catalysis.

References

[1] P. Thenard, C.R. Hebd. *Seances Acad. Sci., Ser. C* (cited in *Modern Coordination Chemistry: the Legacy of Joseph Chatt*, ed. G.J. Leigh, N. Winterton, Royal Society of Chemistry, Cambridge, UK, **2002**), *25* (**1847**).

[2] C.A. Tolman, *Chem Rev*, *77* (**1977**).

II. Ferrocenyl phosphine-type ligands and their transitional metal complexes

II.1. Introduction

Ferrocene-containing compounds were first discovered over 50 years ago and since research into this field continues rapidly, mainly due to applications within catalysis and materials science [1, 2]. Besides its unique structure, ferrocene has ideal properties such as low price, thermal stability, and high tolerance to moisture, oxygen, and many types of reagents. Interestingly, its behaviour as an electron-rich aromatic compound in electrophilic aromatic substitutions, its facile lithiation and dilithiation (at the 1,1'-positions), and the extraordinary ability to stabilize carbocations at the benzylic-like position are key chemical properties that provide very practical ways for the synthesis of functionalized, substituted ferrocenes. In coordination chemistry, the ferrocene moiety has played a significant role as a backbone or a substituent in ancillary ligands due to (i) the specific and unique geometries that the ferrocene provides and (ii) its electronic (redox) properties, whereby the possibility of switching the redox state of the ferrocene backbone gives access to potential control of reactivity at a metal centre.

II.2. Literature overview

The best-known ferrocene ligand, [1,1'-*bis*(diphenylphosphino)ferrocene] (dppf), was first described in 1965 by dilithiation of ferrocene with *n*-butyllithium followed by reaction with chlorodiphenylphosphine. Ever since, dppf and related achiral ferrocenyl phosphines have been successfully and extensively applied in transition-metal catalysed processes [13]. Unlike 1,1'-disubstitution, a very interesting structural feature in ferrocene chemistry is that compounds substituted at positions 1 and 2 with different groups are chiral because of the loss of the plane of symmetry of ferrocene (planar chirality). The ligand ppfa (*N,N*-dimethyl-1-[2-diphenylphosphino) ferrocenyl]ethylamine), synthesized by Hayashi and Kumada in 1974 by *ortho* lithiation of enantiopure (R)-*N,N*-dimethyl- 1-ferrocenylethylamine (Ugi's amine) and reaction with chlorodiphenylphosphine, was the first reported example of a planar-chiral enantiopure ferrocenyl phosphine [13]. The discovery of ppfa and its high efficiency as a chiral ligand in some transition-metal-mediated reactions was a landmark in the development of chiral ferrocene ligands for asymmetric catalysis. Years later, in the 1990s, a breakthrough achievement was the synthesis of the Josiphos family of bisphosphine ferrocene ligands by SN_1-type reaction of the dimethylamino group on Ugi's amine-derived ligands with secondary phosphines (reported by Togni *et al*.) [14].

II.3. Original contributions

II.3.1. Synthesis of monophosphine $FcCH_2P^tBuPh$ (4), phosphonium salt $[(FcCH_2)_2P^tBuPh]^+I^-$ (5) and phosphine oxide $FcCH_2P(O)^tBuPh$ (6)

Although the first ferrocenyl phosphines in which a ferrocene unit is attached directly or through a methylene bridge to the phosphorus atom were prepared a long time ago [48], only a few examples of these phosphines were prepared until the present. In contrast to the great number of ferrocenyl phosphines which have the phosphorus atom directly bonded to the cyclopentadienyl ring, ligands where a carbon atom is situated between these two functionalities are not very well investigated. Developments in this area include hydroxymethylphosphines [33], ferrocenylmethyl-substituted phosphines [49] or ferrocenyl-carboxyphosphines [50].

The target of this work was the synthesis of new chiral ferrocenyl ligands. To accomplish this goal (ferrocenylmethyl)-*t*-buthylphenyl phosphine (**4**) was prepared and characterized. The synthesis of the target ligand was performed starting from *N,N*-dimethylaminomethylferrocene and *t*-butylphenyl phosphine using acetic acid as solvent (**Scheme II.9.**). After 18 h of reflux, the reaction mixture contains the monophosphine **4** and the phosphonium salt (**5**) in a 1:9 molar ratio. Shorter reaction times did not lead to the formation of the desired product, while an increase of the reaction time (41 h reflux) did not improve the yield of the reaction. The formation of the phosphine oxide **6** was also observed.

The NMR spectroscopic analysis indicate a chemical shift of the P atom in phosphine **4** of 7.4 ppm. The two diastereotopic methylene protons appear as two doublets at 2.8 ppm and 3.1 ppm, the P-H coupling constant being $^2J_{PH}$ = 14 Hz. The chemical shift of the P atom of the quaternary phosphonium salt **5** appears in the expected area for this type of compounds, at 30.0 ppm, while the phosphine oxide **6** has the P atom at a chemical shift of 44.9 ppm. The $^3J_{PH}$ coupling constant is 12 Hz for the neutral phosphine **4** and 16 Hz for the cationic phosphonium salt **5**.

The characteristic base peak in the FAB MS spectrum for the phosphonium salt **5** occurs at *m/z* = 199, corresponding to the $FcCH_2^+$ fragment. The molecular peak occurs at *m/z* = 563.2.

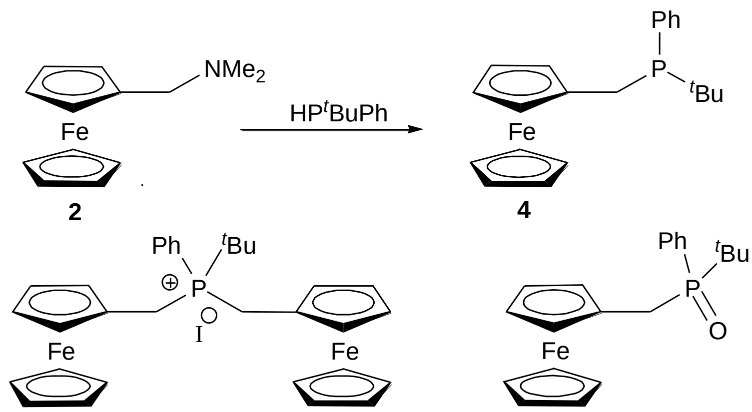

Scheme II.9. Synthesis of monophosphine **4** and the observed byproducts: the phosphonium salt **5** and the phosphine oxide **6**

Phosphine **4** crystallizes in a triclinic crystal system, in $P\bar{1}$ space group with 2 molecules in the unit cell. Some characteristic bond lengths and angles are shown in **Table II.1.** Numbers in parentheses are in the least significant digits. Phosphonium salt **5** crystallizes with one molecule of methanol, in a monoclinic crystal system, in $P2_1/c$ space group with 4 molecules in the unit cell. The solid state molecular structure of phosphine **4** and phosphonium salt **5** are presented in **Fig. II.7** and **Fig. II.8.**, respectively. All hydrogen atoms are omitted for clarity.

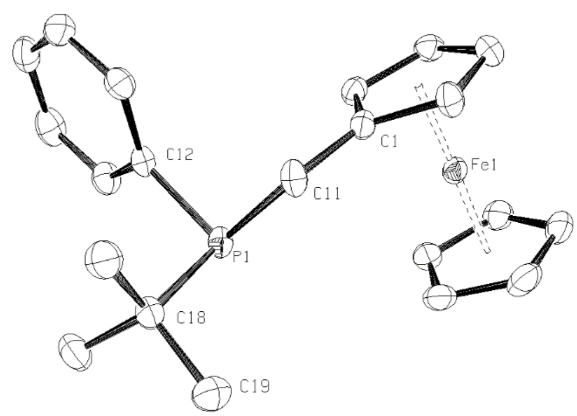

Fig II.7. Solid state molecular structure of (ferrocenylmethyl)-*t*-butylphenyl phosphine (**4**)

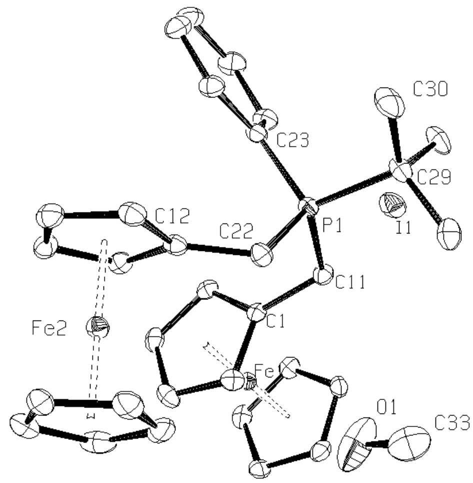

Fig II.8. Solid state molecular structure of phosphonium salt **5**.

Table II.1. Selected bond lengths (Å) and bond angles (°) in **4**

P(1)-C(12)	1.842(2)	C(12)-P(1)-C(11)	102.87(7)
P(1)-C(11)	1.851(2)	C(12)-P(1)-C(18)	101.65(6)
P(1)-C(18)	1.887(2)	C(11)-P(1)-C(18)	100.90(7)
C(18)-C(19)	1.533(2)	C(19)-C(18)-P(1)	106.80(1)
C(1)-C(11)	1.501(2)	C(1)-C(11)-P(1)	115.40(1)

II.2. Synthesis of bisphosphines [1-(^{t}BuPhP)CH_2]-2-(^{t}BuPhP)Fc (9a) and [1-(^{t}BuPhP)CH(CH_3)]-2-(^{t}BuPhP)Fc (9b) and aminophosphine 10

Chiral ferrocenylphosphines possessing planar chirality due to the ferrocene moiety can be prepared by *ortho*-lithiation of the optically resolved *N,N*-dimethyl-1-ferrocenylethylamine [54]. The lithiation of ferrocenylamine with BuLi generates the two possible diastereoisomers in a ratio of 96 to 4. Following the reaction with the electrophile, the diastereoisomeric side-product is usually easily separated by crystallization and/or chromatography [55]. In the next step, the amino group is substituted in acetic acid with a phosphinic group, yielding a bisphosphine bearing planar and central chirality.

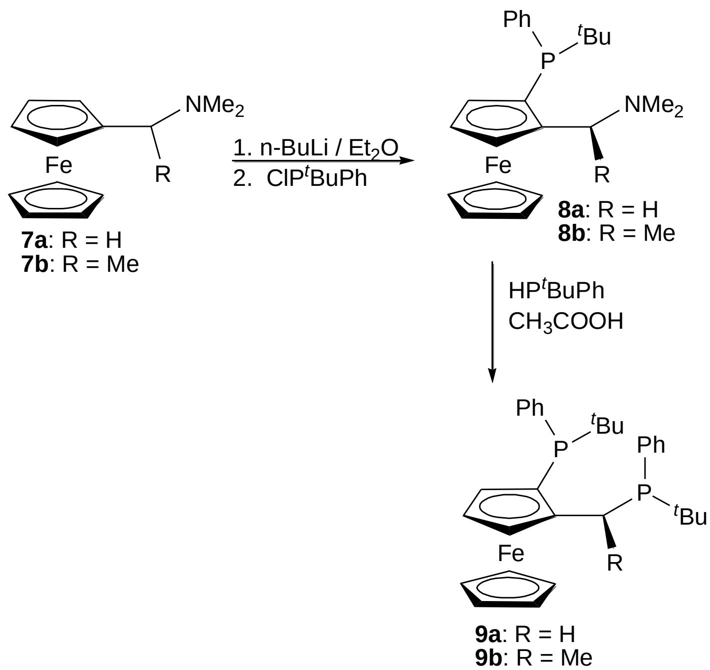

Scheme II.10. Synthesis of bisphosphines **9a** and **9b**

Starting from ferrocenylamine **7a**, in the reaction with *n*-BuLi followed by addition of the electrofile ClP^tBuPh two chirality centres were introduced in a single step so a mixture of four diastereomers was expected [55] (**Scheme II.10.**). A ^{31}P-NMR spectrum of the raw product shows two signals, at 1 and -2.7 ppm in a 1:4 ratio. The solid state structure shows that the stereoselectivity of the synthesis is determined by the steric interactions at the phosphorus atom. Because the *t*-butyl group is very bulky it is positioned in the less hindered conformation and that is above the cyclopentadienyl ring. The phenyl group is below this ring, and rotated in such a way that the reciprocal effects are minimized. Reacting further the aminophosphine **8a** with HP^tBuPh in acetic acid, the amino group is replaced by a phosphino group, yielding bisphosphine **9a**. A diastereomeric mixture is obtained, but 3 types of racemic mixtures were fractionally crystallized from ethanol. The first pair of enantiomers which crystallizes has in ^{31}P-NMR the chemical shifts δ_{P1} = -3.9 ppm and δ_{P2} = 4.5 ppm. These chemical shifts correspond to the configuration $P^1_S\ P^2_S\ Fc_R$ / $P^1_R\ P^2_R\ Fc_S$. This configuration was confirmed by X-ray measurements on a single crystal. The other two pairs of enantiomers have the chemical shifts δ_{P1} = -1.8 ppm, δ_{P2} = 2.4 ppm and δ_{P1} = -3.2 ppm, δ_{P2} = 1.6 ppm respectively. In solution all 4 pairs of enantiomers are observed, due to the fact that in solution isomerization occurs. After crystallizing one pair of enantiomers, the ^{31}P-NMR spectrum of the solution of the diastereomeric mixture shows that all diastereomers are present again.

The EI-MS spectra shows the base peak at *m/z* = 471.1 corresponding to the loss of one *t*-butyl group ($[M - {}^tBu]^+$). The loss of the second *t*-butyl group is also observed at *m/z* = 414.1. In addition a peak corresponding to $[C_5H_5FeC_5H_3\text{-}CH{=}P\text{-}Ph]^+$ can also be seen (*m/z* = 305), along with *m/z* = 121 for $[HC{=}P\text{-}Ph]^+$. Characteristic for this type of compounds is the peak *m/z* = 199 corresponding to $FcCH_2^+$. In the MS-ESI spectrum, the molecular peak can be found at *m/z* = 529 (M+1).

The solid state molecular structure of bisphosphine **9a** is shown in **fig. II.9**. Only one enantiomer is shown (P^1_S P^2_S Fc_R). Compound **9a** crystallizes in space group $P\bar{1}$, in a triclinic crystal system with 2 molecules in the unit cell. The determined structure belongs to the racemic mixture P^1_S P^2_S Fc_R / P^1_R P^2_R Fc_S. Some characteristic bond lengths and angles are presented in **Table II.3**. Numbers in parentheses are in the least significant digits. These are in agreement with the bond lengths and angles measured in the case of similar compounds [47, 56]. In the case of bisphosphine **9a**, the C-P-C angles are slightly wider because of the bulky *t*-butyl substituent compared to another phenyl group in a Josiphos type ligand (R = Ph, R' = Cy; 107.24° compared to 100.5° in Josiphos ligand).

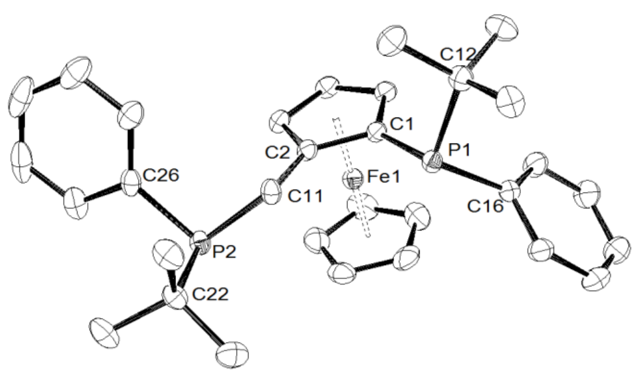

Fig. II.9. Molecular structure of $[1\text{-}({}^tBuPhP)CH_2]\text{-}2\text{-}({}^tBuPhP)Fc$ (**9a**). Thermal ellipsoids are drawn at 50% probability. The hydrogen atoms are omitted for clarity. Only one enantiomer is shown (P^1_S P^2_S Fc_R).

Table II.3. Selected bond lengths (Å) and bond angles (°) in **9a**

P(1)-C(1)	1.813(1)	C(12)-P(1)-C(16)	104.36(6)
P(1)-C(12)	1.872(1)	C(16)-P(1)-C(1)	107.24(6)
P(1)-C(16)	1.828(1)	C(12)-P(1)-C(1)	104.32(6)
P(2)-C(11)	1.843(1)	C(11)-P(2)-C(22)	99.46(6)
P(2)-C(26)	1.835(1)	C(26)-P(2)-C(22)	102.38(6)

P(2)-C(22)	1.883(1)	C(11)-P(2)-C(26)	103.09(6)
C(2)-C(11)	1.499(2)	C(2)-C(11)-P(2)	116.71(9)

The first palladium catalysed C-C coupling reaction was realized in 1979 [58] and since then this field has greatly developed, allowing to perform open-air oxidative Heck reactions at room temperature [59] or synthesis of new P-C bonds [60]. Based on the good results that Josiphos type ligands showed in the palladium-catalysed C-C coupling reactions, the catalytic activity of ligand **9a** was tested in the coupling reaction of *t*-butyl acrylate with phenyl bromide (**Scheme II.11.**).

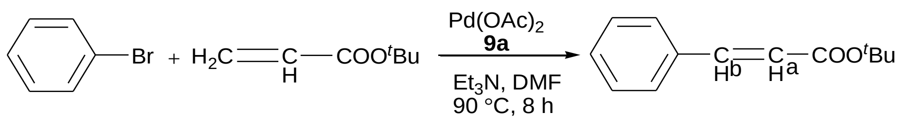

Scheme II.11. Heck coupling of *t*-butyl acrylate with phenyl bromide

The catalyst was prepared in situ by heating ligand **9a** with palladium acetate for 30 min at 40 °C, then the substrates were added in a 1/100 molar ratio (catalyst/substrate). After removal of the catalyst, the formation of the target compound can be observed in the ^{1}H-NMR spectra of mixture. The detail in **Fig. II.10.** shows the two protons of the vinyl unit: H^a at 5.80 ppm while H^b has the chemical shift 6.78 ppm. Considering that the $^3J_{HH}$ coupling constant is 12 Hz, we can conclude that the *cis* isomer of the product is obtained. Based on the ^{1}H-NMR spectra, the conversion was only 6% in these reaction conditions.

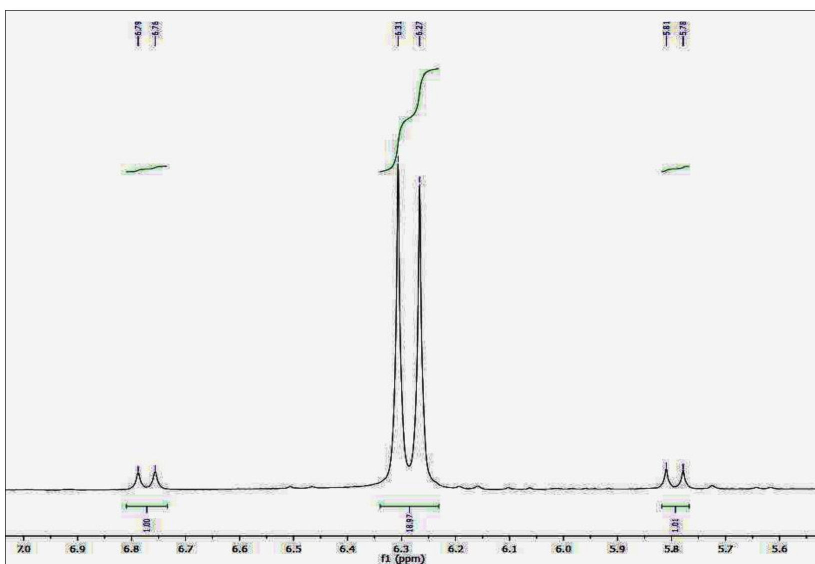

Fig. II.10. ^{1}H-NMR (detail) of the reaction mixture after 8 h at 90 °C of Heck coupling of *t*-butyl acrylate with phenyl bromide in the presence of **9a**

Based on the previously shown results regarding the synthesis and isolation of the diastereomers (R, R / S, S), the same reaction was performed starting from the C-chiral aminoferrocene **7b** [55] (**Scheme II.10.**). The raw product showed in this case also a mixture of two diastereomers in a 1:4 ratio. The major diastereomer was fractionally crystallized from ethanol. The structure belonging to the chiral space group *P1*, shows as in the case of the previous compound no specific bond length and angles. Comparing this compound to ppfa (which has the same structure but has a phenyl group instead of the *t*-butyl group), in the case of compound **8b** the P-C bonds are longer and the C-P-C angles are larger because of the bulkiness of the *t*-butyl group. When diastereomerically pure **8b** was reacted at reflux with HP^tBuPh in acetic acid, it did not retain completely its stereochemistry, epimerization occurred at the P atom due to the high temperature (120 °C) required for the reaction. Enantiomerically pure **9b** was obtained by fractional crystallization in ethanol, bearing 4 chirality elements (planar chirality, central chirality at two phosphorus atoms and a carbon atom).

Starting from C_R P_S Fc_S aminophosphine **8b**, after 4 h reflux in acetic acid in the presence of HP^tBuPh, C_R P^1_R P^2_S Fc_S **9b** was obtained. The stereochemistry of the carbon atom remains the same, but the stereochemistry of the already existing phosphorus atom is reversed. In the ^{31}P-NMR spectrum the chemical shifts of the phosphorus atoms are δ_{P1} = -2.5 ppm and δ_{P2} = 22.0 ppm.

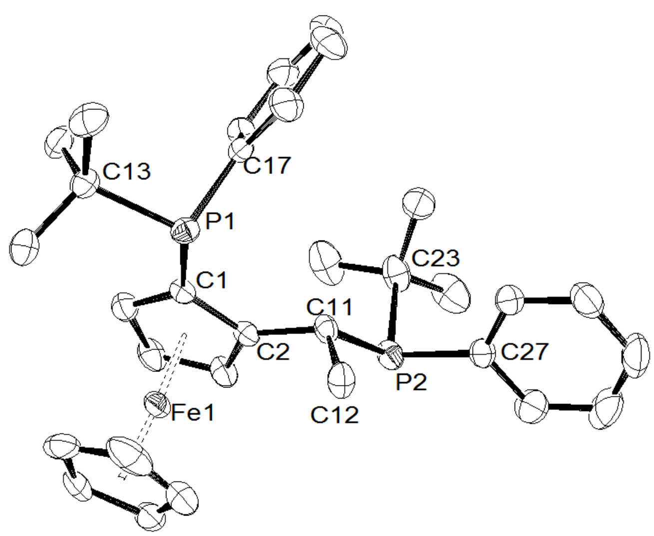

Fig. II.11. ORTEP diagram of [1-(^{t}BuPhP)CH(CH_3)]-2-(^{t}BuPhP)Fc (**9b**). Thermal ellipsoids are drawn at 50% probability. All hydrogen atoms are omitted for clarity.

Bisphosphine **9b** crystallizes in an orthorhombic crystal system, in the chiral space group $P2_12_12_1$ with 4 molecules in the unit cell. Its solid state molecular structure is presented in **Fig. II.11**. The absolute structure parameter, also known as Flack parameter, has the value -0.004(10). This is characteristic to compounds that crystallize in an enantiomerically pure form. Selected bond distances and angles are found in **Table II.4**.

Table II.4. Selected bond lengths (Å) and bond angles (°) in **9b**

P(1)-C(1)	1.823(2)	C(13)-P(1)-C(17)	100.31(8)
P(1)-C(17)	1.835(2)	C(17)-P(1)-C(1)	100.47(8)
P(1)-C(13)	1.886(2)	C(13)-P(1)-C(1)	106.92(8)
P(2)-C(11)	1.875(2)	C(11)-P(2)-C(23)	106.07(9)
P(2)-C(27)	1.835(2)	C(27)-P(2)-C(23)	100.02(9)
P(2)-C(23)	1.901(2)	C(11)-P(2)-C(27)	102.87(8)
C(2)-C(11)	1.523(2)	C(2)-C(11)-P(2)	109.8(1)
C(11)-C(12)	1.530(3)		

All bond lengths and angles have similar values with those reported for Josiphos ligand (R = Ph, R' = Cy) [47], or other similar compounds [61, 62] the main difference being a bigger distance between the phosphorus atoms in compound **9b** (5.09 Å) compared to Josiphos (R = Ph, R' = Cy; 3.70 Å). The reason might be the stronger steric repulsions between the bulky *t*-butyl groups than in the case of phenyl-cyclohexyl repulsions.

The bond lengths have similar values in **9a** compared to **9b,** with small differences of only 0.01-0.02 Å, the only notable differences are that introducing a methyl group attached to C(11), the P(2)-C(11) and C(2)-C(11) bonds become longer with 0.03 Å and 0.02 Å respectively. The angles in the two ligands have comparable values, the smallest difference being of 0.22° (in the case of C(11)-P(2)-C(26) compared to the corresponding C(11)-P(2)-C(27) angle); the most outstanding difference can be observed in the case of C(2)-C(11)-P(2) of 6.91°, this angle being smaller in the case of ligand **9b**, which has a methyl group attached to C(11). The distances between the phosphorus atoms are similar: 4.909 Å in **9a** and 5.094 Å in **9b**.

The MS-EI spectra shows some characteristic fragments for this type of compounds. The loss of one (*m/z* 484.9 $[M - {}^tBu]^+$) or two (*m/z* 427.9 $[M - 2\,{}^tBu]^+$) *t*-butyl groups can be observed. The base peak can be found at *m/z* = 318.9 corresponding to $[C_5H_5FeC_5H_3\text{-}C(CH_3)\text{=}P\text{-}Ph]^{\cdot+}$, along with *m/z* = 120.9 for $[HC\text{=}P\text{-}Ph]^+$. In the MS-ESI spectrum the molecular peak can be found at m/z = 543.1 (M+1).

The synthesis of ferrocenyl 1,2-bisphosphines bearing oxazaphospholidine substituents was experimentally performed. The intermediate (aminomethyl)-ferrocenyl-phosphine **10** was obtained in the reaction of *N,N*-dimethylaminomethylferrocene and 3-*t*-butyl-2-chloro-1,3,2-oxazaphospholidine in diethyl ether (**Scheme II.12.**). Unfortunately, the 1,2-bisphosphine **11** could not be obtained based on this reaction sequence.

10 was obtained as a brown oil and could not be thoroughly purified. The ^{1}H and ^{31}P-NMR of the compound were recorded. The chemical shift of the phosphorus atom is 156.5 ppm. Compound **10** was further reacted with HP^{t}BuPh in acetic acid in the attempt of synthesizing bisphosphine **11**. Unfortunately, compound **10** decomposes in acetic acid, even at room temperature.

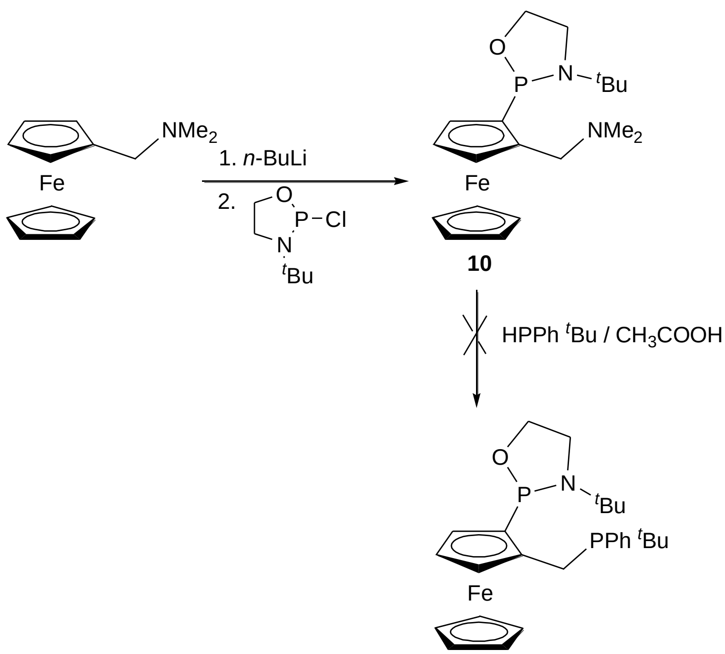

10

11

Scheme II.12. Synthesis of (aminomethyl)-ferrocenyl-phosphine **10**

II.3.3. Synthesis of [PdCl$_2${[1-(^{t}BuPhP)CH$_2$]-2-(^{t}BuPhP)Fc}] (12a) and [PdCl$_2${[1-(^{t}BuPhP)CH(CH$_3$)]-2-(^{t}BuPhP)Fc}] (12b)

Understanding of the coordination behaviour of these ligands with a variety of transition metals is vital as it gives the basic information about the reactivity, the stability and the steric and electronic situation around the metal centre. To accomplish this goal, palladium complexes, **12a** and **12b**, of the synthesized 1,2-bisphosphines **9a** and **9b**, were prepared. The synthesis of these complexes is based on the ability of the phosphorus atom to coordinate to a metal centre. **9a** and **9b**, respectively were treated with [PdCl$_2$(cod)] in dichloromethane. (**Scheme II.13.**).

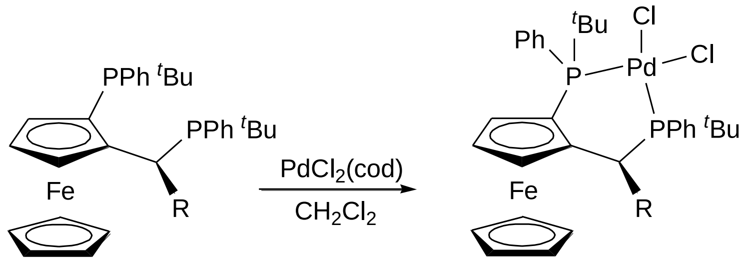

9a: R = H
9b: R = Me

12a: R = H
12b: R = Me

Scheme II.13. Synthesis of palladium complexes **12a** and **12b**

The products were characterized by ^{1}H and ^{31}P-NMR. Since the phosphorus atoms are not equivalent, two peaks were observed in the ^{31}P-NMR spectrum, with signals shifted downfield compared to the free phosphines. There are very small differences between the chemical shifts of the phosphorus atoms in complexes **12a** and **12b**. While the chemical shifts for the P atoms in **12a** are 39.7 ppm and 83.4 ppm, respectively, the phosphorus atoms of complex **12b** can be observed in the ^{31}P-NMR at 39.3 ppm and 83.8 ppm, respectively. For similar compounds, $^2J_{PP}$ coupling constants were observed [42], their values being in the range of 10-20 Hz, suggesting that both phosphorus atoms were bonded to the Pd(II). In the case of other reported compounds coupling could not observed and the signals occurred unresolved. This is the case of complexes **12a** and **12b** also, where one ^{31}P signal is a sharp singlet while the other one is broad. The fact that both phosphorus atoms coordinate to the palladium atom was proven by X-ray measurements. While complex **12b** was crystallized from dichloromethane, red plates of **12a** were obtained from a mixture of dichloromethane and diethyl ether. Complex **12a** crystallizes in $P2_1/c$ space group with 4 molecules in the unit cell. The units of **12a** also contain two molecules of dichloromethane per molecule of complex. Complex **12b** crystallizes in a monoclinic crystal system, in space group $P2_1$ with 2 molecules in the unit cell. 3 molecules of dichloromethane per molecule of complex **12b** are also found in the unit cell. Coordination to the Pd atom occurs with retention of configuration. **Fig. II.12.** presents the solid state molecular structure of complex **12a**.

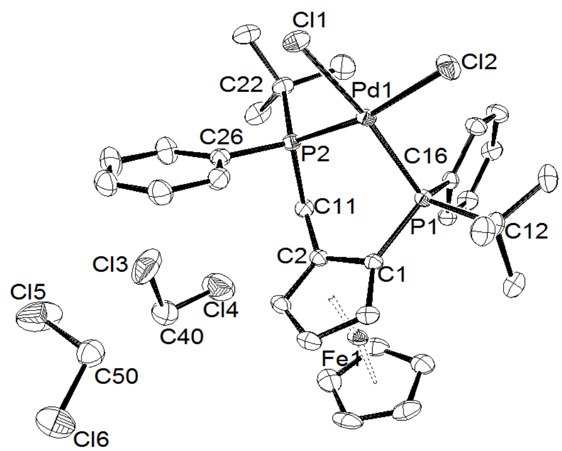

Fig. II.12. ORTEP diagram of $[PdCl_2\{[1-(^tBuPhP)CH_2]-2-(^tBuPhP)Fc\}]$ (**12a**).

Some selected bond lengths and angles of compound **12a** are presented in **Table II.5**. In the free ligand **9a**, the distance between the two phosphorus atoms is 4.909 Å, compared to a smaller value due to coordination (3.303 Å in complex **12a**). Data collections and structure analysis details are presented in **Appendix 2** (*see* A 2.5).

Table II.5. Selected bond lengths (Å) and bond angles (°) in **12a**

P(1)-C(1)	1.806(2)	C(1)-P(1)-C(12)	106.32(9)
P(1)-C(16)	1.809(2)	C(12)-P(1)-C(16)	103.62(9)
P(1)-C(12)	1.875(2)	C(1)-P(1)-C(16)	111.17(9)
P(1)-Pd	2.2782(5)	C(1)-P(1)-Pd	106.51(6)
P(2)-C(11)	1.833(2)	C(16)-P(1)-Pd	107.95(6)
P(2)-C(22)	1.873(2)	C(12)-P(1)-Pd	121.21(7)
P(2)-C(26)	1.812(2)	C(2)-C(11)-P(2)	108.3(1)
C(2)-C(11)	1.484(3)	C(11)-P(2)-C(26)	102.88(9)
P(2)-Pd	2.2680(5)	C(11)-P(2)-C(22)	103.41(9)
Pd-Cl(1)	2.3500(5)	C(26)-P(2)-C(22)	111.15(9)
Pd-Cl(2)	2.3358(5)	C(22)-P(2)-Pd	112.17(7)
		C(26)-P(2)-Pd	111.78(7)
		C(11)-P(2)-Pd	114.84(6)
		P(1)-Pd-P(2)	93.21(2)
		P(1)-Pd-Cl(2)	94.47(2)
		P(2)-Pd-Cl(1)	85.58(2)
		Cl(1)-Pd-Cl(2)	88.46(2)

The structure of complex **12b** was also determined by X-ray diffraction. Starting from the enantiomerically pure ligand **9b**, only one enantiomer of the palladium complex **12b** is obtained, the absolute structure parameter having the value -0.009(11). The solid state molecular structure of complex **12b** is shown in **Fig. II.13.**, while selected bond lengths and angles are presented in **Table II.6**.

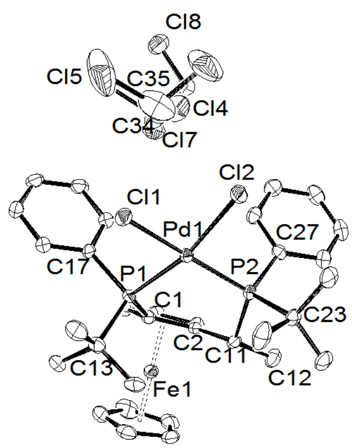

Fig. II.13. ORTEP diagram of $[PdCl_2\{[1-(^tBuPhP)CH(CH_3)]-2-(^tBuPhP)Fc\}]\cdot3CH_2Cl_2$ (**12b**).

Complex **12b** crystallizes with 3 molecules of CH_2Cl_2. The palladium atom has a distorted planar geometry, while the two phosphorus atoms are situated in a tetrahedral environment. The distance between the two phosphorus atoms in complex **12b** is 4.162 Å, compared to 5.094 Å in the uncoordinated ligand **9b**. Compared to other palladium complexes of Josiphos ligands [42, 46], the bond lengths and angles differ slightly depending on the substituents of the phosphorus atom. The P-C bonds are longer (0.03-0.05 Å) in the case of complexes **12a** or **12b**, having only one ^{t}Bu group on one P atom compared to complexes bearing two ^{t}Bu groups but smaller compared to complexes in which the P atom has only phenyl groups as substituents. These differences are likely due to the more sterically demanding ^{t}Bu groups. The bond lengths have similar values in the complexes and the free ligands, but the angles are up to 11° wider in the complexes compared to the ligands, probably due to the rigidity of the structures. For example, C(13)-P(1)-C(17) is 100.31(8)° in **9b** but 111.3(1)° in **12b**.

Table II.6. Selected bond lengths (Å) and bond angles (°) in **12b**

P(1)-C(1)	1.799(3)	C(1)-P(1)-C(13)	109.2(1)
P(1)-C(13)	1.855(3)	C(13)-P(1)-C(17)	111.3(1)
P(1)-C(17)	1.826(3)	C(1)-P(1)-C(17)	100.1(1)

P(1)-Pd	2.2626(7)	C(1)-P(1)-Pd	112.67(9)
P(2)-C(11)	1.878(3)	C(17)-P(1)-Pd	104.08(9)
P(2)-C(23)	1.892(3)	C(13)-P(1)-Pd	117.9(1)
P(2)-C(27)	1.817(3)	C(2)-C(11)-P(2)	110.3(2)
C(2)-C(11)	1.516(4)	C(11)-P(2)-C(27)	103.7(1)
C(11)-C(12)	1.536(4)	C(11)-P(2)-C(23)	106.8(1)
P(2)-Pd	2.2878(7)	C(27)-P(2)-C(23)	110.7(1)
Pd-Cl(1)	2.3519(7)	C(12)-C(11)-P(2)	115.0(2)
Pd-Cl(2)	2.3537(7)	C(23)-P(2)-Pd	109.22(9)
		C(27)-P(2)-Pd	110.52(9)
		C(11)-P(2)-Pd	115.68(8)
		P(1)-Pd-P(2)	97.90(3)
		P(1)-Pd-Cl(2)	165.75(3)
		P(2)-Pd-Cl(1)	172.97(3)
		Cl(1)-Pd-Cl(2)	86.33(2)

II.3.4. Synthesis of [RhCl{[1-(^{t}BuPhP)CH(CH_3)]-2-(^{t}BuPhP)Fc}]$_2$ (13)

The Josiphos ligands incorporate a transition metal containing unit as the central core around which the ligand framework is constructed. This transition metal itself is not involved in the catalysis, but is part of the scaffold to which the ligand functions are attached. The function of the metal is to create a chiral environment, the spatial and dynamic properties of which could not be achieved by an organic framework alone. Rhodium complexes of bisphoshines have found applications in organic reactions like asymmetric hydrogenations [65, 66] or acetalization reactions [67].

To study the coordination chemistry of the newly synthesized ferrocenyl bisphosphines, ligand **9b** was reacted with [$RhCl_2$(cod)]$_2$ in a 2:1 molar ratio (**Scheme II.14.**).

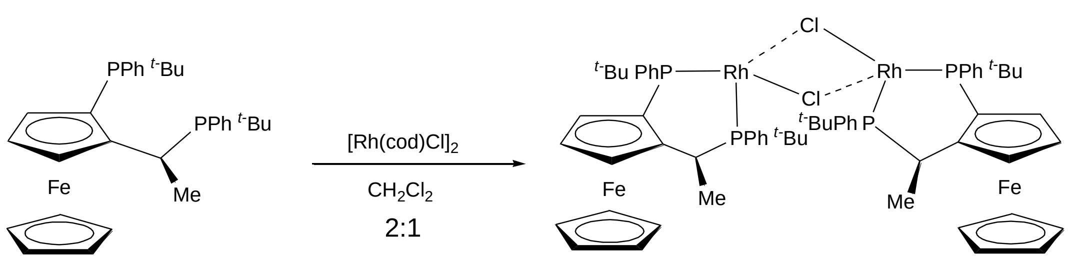

9b **13**

Scheme II.14. Synthesis of rhodium complex **13**

The ^{31}P-NMR spectra of compound **13** shows a set of two double doublets, at 49.1 ppm and 58.9 ppm, respectively, revealing a P,P coupling constant of 43 Hz and a $^{1}J_{RhP}$ = 114.35 Hz. This can be due to the fact that upon complexation the two phosphorus atoms become synperiplanar. Similar results were obtained in the case of other ferrocenyl bisphosphines [56].

II.3.5. Conclusions

(Ferrocenylmethyl)-*t*-butylphenyl phosphine (**4**) was prepared by nucleophilic substitution starting from amine **2** and ammonium salt **3**. As byproducts, phosphonium salt **5** and phosphineoxide **6** were obtained and characterized.

Synthesis of ferrocenyl-1,2-bisphosphines [1-(^{t}BuPhP)CH_2]-2-(^{t}BuPhP)Fc (**9a**) and [1-(^{t}BuPhP)CH(CH_3)]-2-(^{t}BuPhP)Fc (**9b**) was performed starting from the corresponding ferrocenylmethyl-amines **7a** and **7b**, respectively. The catalytic activity of ligand **9a** was tested in a palladium-catalyzed Heck coupling reaction.

Oxazaphospholidin-aminomethyl-ferrocene **10** was obtained in the reaction of *N,N*-dimethylaminomethylferrocene and 3-*tert*-butyl-2-chloro-1,3,2-oxazaphospholidine.

Synthesis of palladium complexes of ferrocene-1,2-bisphosphines [$PdCl_2${[1-(^{t}BuPhP)CH_2]-2-(^{t}BuPhP)Fc}] (**12a**) and [$PdCl_2${[1-(^{t}BuPhP)CH(CH_3)]-2-(^{t}BuPhP)Fc}] (**12b**) was performed starting from the already synthesized ligands **9a** and **9b**.

Ligand **9b** and palladium complex **12b** were obtained in an enantiomerically pure form, although 4 chirality elements are present in the molecular structures. The solid state structures of the crystallized compounds were compared to similar structures from the literature and no abnormalities were found.

The coordination properties of ligand **9b** were studied towards Rh, and based on the ^{31}P-NMR spectrum a structure for complex **13** was proposed.

References

[1] A. Togni, T. Hayashi, Ferrocenes. *Homogeneous Catalysis-Organic Synthesis-Material Science*, VCH, Weinheim, Germany, **1995**.

[2] N.J. Long, *An Introduction to Sandwich Complexes*, Blackwell Science, Oxford, **1998**.

[3] J.C. Jeffrey, T.B. Rauchfuss, *Inorg. Chem*., *18* (**1979**) 2658.

[4] C.S. Slone, D.A. Weinberger, C.A. Mirkin, *Prog. Inorg. Chem*., *48* (**1999**) 233.

[5] J.R. Dilworth, N. Wheatley, *Coord. Chem. Rev*., *199* (**2000**) 89.

[6] A. Bader, E. Lindner, *Coord. Chem. Rev*., *108* (**1991**) 27.

[7] J. Ansell, M. Wills, *Chem. Soc. Rev*., *31* (**2002**) 259.

[8] G. Helmchen, A. Pfaltz, *Acc. Chem. Res*., *33* (**2000**) 336.

[9] G. Helmchen, S. Kudis, P. Sennham, H. Steinhagen, *Pure Appl. Chem*., *69* (**1997**) 513.

[10] S.Y. Desjardins, K.J. Cavell, J.L. Hoare, B.W. Skelton, A.N. Sobolev, A.H. White, W. Keim, *J. Organomet. Chem*., *544* (**1997**) 163.

[11] C. Wang, S. Friedrich, T.R. Younkin, R.T. Li, R.H. Grubbs, D.A. Bansleben, M.W. Day, *Organomet.*, *17* (**1998**) 3149.

[12] F.A. Hicks, M. Brookhart, *Organomet*., *20* (**2001**) 3217.

[13] T. Hayashi, K. Yamamoto, M. Kumada, *Tetrahedron Lett*., (**1974**) 4405.

[14] A. Togni, C. Breutel, A. Schneyder, F. Spindler, H. Landert, A. Tiijani, J*. Am. Chem. Soc.*, *116* (**1994**) 4062.

[15] T.J. Colacot, *Chem. Rev*., *103* (**2003**) 3101.

[16] T. Hayashi, M. Tajika, K. Tamao, M. Kumada, *J. Am. Chem. Soc*., *98* (**1976**) 3718.

[17] C. Bolm, K. Muniz-Fernandez, K. Segerer, G. Raabe, K. Gunther, *J. Org. Chem*., *63* (**1998**) 7860.

[18] S.L. You, X.L. Hou, X.L. Dai, Y.H. Yu, W. Xia, *J. Org. Chem*., *67* (**2002**) 4684.

[19] R.C.J. Atkinson, V.C. Gibson, N.J. Long, *Chem. Soc. Rev*., *33* (**2004**) 313.

[20] I.R. Butler, W.R. Cullen, T.J. Kim, S.J. Rettig, J. Trotter, *Organomet.*, *4* (**1985**) 972.

[21] J.A. Adeleke, Y.W. Chen, L.K.Liu, *Organomet*., *11* (**1992**) 2543.

[22] L.L. Lai, T.Y. Dong, J. Chem. Soc., *Chem. Commun*., (**1994**) 2347.

[23] I.R. Butler, R.L. Davies, *Synthesis*, (**1996**) 1350.

[24] J.M. Chong, L.S. Hegedus, *Organomet*., *23* (**2004**) 1010.

[25] D. Marquarding, H. Klusacek, G. Gokel, P. Hoffmann, I. Ugi, *J. Am. Chem. Soc*., *92* (**1970**) 5389.

[26] W. Magerlein, A.F. Indolese, M. Beller, *Angew. Chem. Int. Ed. Engl*., *40* (**2001**) 2856.

[27] C. Gambs, S. Chaloupka, G. Consiglio, A. Togni, *Angew. Chem. Int. Ed*., *39* (**2000**) 2486.

[28] H.C.L. Abbenhuis, U. Burckhardt, V. Gramlich, C. Köllner, P.S. Pregosin, R. Salzmann, A. Togni, *Organomet*., *14* (**1995**) 759.

[29] A.H. Roy, J.F. Hartwig, *J. Am. Chem. Soc*., *125* (**2003**) 8704.

[30] C.G. Leong, O.M. Akotsi, M.J. Ferguson, S.H. Bergens, *Chem Commun*., (**2003**) 750.

[31] M. Lautens, S. Hiebert, J.L. Renaud, *Org. Lett*., *2* (**2000**) 1971.

[32] H.U. Blaser, H.P. Buser, R. Hausel, H.P. Jalett, F. Spindler, *J. Organomet. Chem*., *621* (**2001**) 34.

[33] J.F. Buergler, A. Togni, *Chem Commun*., *47* (**2011**) 1896.

[34] V.V. Dunina, O.N. Gorunova, M.V. Livantsov, Y.K. Grishin, L.G. Kuz'mina, N.A. Kataeva, A.V. Churakov, *Inorg. Chem. Commun*., *3* (**2000**) 354.

[35] N.J. Goodwin, W. Henderson, *Polyhedron*, *17* (**1998**) 4071.

[36] N.J. Goodwin, W. Henderson, J.K. Sarfo, *Chem Commun*., (**1996**) 1551.

[37] D.A. Redfield, L.W. Cary, J.H. Nelson, *Inorg. Chem*., *14* (**1975**) 50.

[38] D.A. Redfield, J.H. Nelson, *Inorg. Nucl. Chem. Lett*., *10* (**1974**) 727.

[39] N.J. Goodwin, W. Henderson, B.K. Nicholson, *Inorg. Chim. Acta*, *295* (**199**9) 18.

[40] A. Togni, F. Spindler, G. Rihs, N.C. Zanetti, M.C. Soares, T. Gerfin, V. Gramlich, *Inorg. Chim. Acta*, *222* (**1994**) 213.

[41] N.C. Zanetti, F. Spindler, J. Spencer, A. Togni, G. Rihs, *Organomet.*, *15* (**1996**) 860.

[42] B.L. Ghent, S.L. Martinak, L.A. Sites, J.A. Golen, A.L. Rheingold, C. Nataro, *J. Organomet. Chem*., *692* (**2007**) 2365.

[43] B.H. Lipshutz, K. Noson, W. Chrisman, A. Lower, *J. Am. Chem. Soc*., *125* (**2003**) 8779.

[44] T.J. Brunker, N.F. Blank, J.R. Moncarz, C. Scriban, B.J. Anderson, D.S. Glueck, L.N. Zakharov, J.A. Golen, R.D. Sommer, C.D. Incarvito, A.L. Rheingold, *Organomet*., *24* (**2005**) 2730.

[45] M. Sperrle, G. Consiglio, *J. Am. Chem. Soc*., *117* (**1995**) 12130.

[46] C. Gambs, G. Consiglio, A. Togni, *Helv. Chim. Acta*, *81* (**2001**) 3105.

[47] A. Togni, C. Breutel, M.C. Soares, N. Zanetti, T. Gerfin, V. Gramlich, F. Spindler, G. Rihs, *Inorg. Chim. Acta*, *222* (**1994**) 3205.

[48] P.L. Pauson, W.E. Watts, *J. Chem. Soc*., (**1963**) 2990.

[49] R. Kalio, P. Lönnecke, E. Hey-Hawkins, *J. Organomet. Chem*., *693* (**2008**) 590.

[50] M. Lamač, I. Císařová, P. Štěpnička, *J. Organomet. Chem*., *690* (**2005**) 4285.

[51] G. Marr, T.M. White, *J. Chem. Soc., Perkin Trans 1*, (**1973**) 1955.

[52] D. Lednicer, C.R. Hauser, *Org. Synth., Coll. Vol. 5* (**1973**) 434.

[53] N.J. Goodwin, W. Henderson, B.K. Nicholson, J.K. Safro, J. Fawcett, D.R. Russell, *J. Chem. Soc., Dalton Trans.*, (**1997**) 4377.

[54] T. Hayashi, T. Mise, M. Fukushima, M. Kagotani, N. Nagashima, Y. Hamada, A. Matsumoto, S. Kawakami, M. Konishi, K. Yamamoto, M. Kumada, *Bull. Chem. Soc. Jpn*., *53* (**1980**) 1138.

[55] S. Tschirschwitz, *PhD Thesis*, University of Leipzig, **2007**.

[56] W. Braun, B. Calmuschi, J. Haberland, W. Hummel, A. Liese, T. Nickel, O. Stelzer, A. Salzer, *Eur. J. Inorg. Chem*., (**2004**) 2235.

[57] J. McGarrity, F. Spindler, R. Fuchs, M. Eyer, in: *Chem. Abstr*., *122*, (**1995**), P81369q.

[58] R.F. Heck, *Acc. Chem. Res*., *12* (**1978**) 146.

[59] P.A. Enquist, J. Lindh, P. Nilsson, M. Larhed, *Green Chem*., *47* (**2006**) 4878.

[60] P. Butti, R. Rochat, A.D. Sadow, A. Togni, *Angew. Chem. Int. Ed*., *47* (**2008**) 4878.

[61] F.H. Allen, O. Kennard, D.G. Watson, L. Brammer, A.G. Orpen, R. Taylor, J*. Chem. Soc., Perkin Trans. II*, (**1987**) suppl. S1-S19.

[62] G.A. Orpen, L. Brammer, F.H. Allen, O. Kennard, D.G. Watson, R. Taylor, *J. Chem. Soc., Dalton Trans.*, (**1989**) suppl. S1-S83.

[63] I. Suisse, H. Bricout, A. Mortreux, *Tetrahedron Lett*., *35* (**1994**) 413.

[64] H. Bricout, J.F. Carpentier, A. Mortreux, *Tetrahedron Lett*., *37* (**1996**) 6105.

[65] I.N. Houpis, L.E. Patterson, C.A. Alt, J.R. Rizzo, T.Y. Zhang, M.Haurez, *Org. Lett*., *7* (**2005**) 1947.

[66] A. Korostylev, V. Andrushko, N. Andrushko, V.I. Tararov, G. König, A. Börner, *Eur. J. Org. Chem*., (**2008**) 840.

[67] P. Barbaro, C. Bianchini, W. Oberhauser, A. Togni, *J. Mol. Catal. A: Chem*., *145* (**1999**) 139.

[68] S. Kohn, *PhD Thesis*, Leizpig University, **2006**.

[69] G.W. Gokel, I.K. Ugi, *J. Chem. Educ*. (modified procedure), *49* (**1972**) 294.

[70] S. Schweizer, J.M. Becht, C.L. Drian, *Org. Lett*., *9* (**2007**) 3777.

[71] S.D. Pastor, J.L. Hyun, P.A. Odorisio, R.K. Rodebough, *J. Am. Chem. Soc*., *11*0 (**198**8) 6547.

[72] F.A. Cotton, *Inorg. Synth*., *13* (**1972**) 52.

[73] G. Giordano, R.H. Crabtree, R.M. Heintz, D. Forster, D.E. Morris, *Inorg. Synth*., *28* (**1990**) 88.

[74] SMART: Area-Detector Software Package, Siemens Industrial Automation, Inc., Madison, WI, **1993**.

[75] G.M. Sheldrick, SHELXS-97, Program for Crystal Structure Solution, Göttingen, **1997**.

[76] G.M. Sheldrick, SHELXL-97, Program for the Refinement of Crystal Structures, Göttingen, **1997**.

[77] G.M. Sheldrick, SADABS, Program for Scaling and Correction of Area-detector Data, University of Göttingen, Germany, **1997**.

[78] L.J. Farrugia, ORTEP3 for Windows, *J. Appl. Crystallogr*., *30* (**1997**) 565.

III. Phenothiazinyl-phosphines and their transitional metal complexes

III.1. Introduction

Because of the high electronegativity of the heterocyclic nitrogen atom, electrophilic substitution reactions are the best method to synthesize *N*-substituted phenothiazines [10]. In the case of *N*-alkyl substituted phenothiazines, delocalization of the nitrogen lone pair electrons is decreased; consequently the reactivity of these compounds towards electrophilic substitution reactions is lower.

III.2. Literature overview

Research in the field of bisphosphine ligands based on heterocyclic aromatic backbones developed fast because of their applications in a great variety of catalysed processes. Since the synthesis of Xantphos [23], many similar ligands have been developed and used with success in catalysis (*e.g*. hydroformylation [24, 25] or asymmetric allylic alkylation [26]) due to their large bite angle. Because the effects of Pd(II) complexes containing ligands inducing wide bite-angles based on xanthene backbones on catalysis are not completely understood, van Leeuwen *et al* [27] have changed the electronic and steric properties of these ligands to study the effects on the geometry of the Pd(II) complexes. There are only few examples of monophosphines with a xanthene-type backbone [28-30], which have found applications in telomerisation of buta-1,3-diene and methanol.

III.3. Original contributions

III.3.1. Synthesis of phenothiazinyl-phosphites

The first attempt of synthesizing a phenothiazinyl-phosphite is presented in **Scheme III.4.** 3-Bromo-10-methyl-phenothiazine **14a** was lithiated at low temperature (addition of *n*-BuLi was made at -78 °C during 30 minutes than it was additionally stirred for half an hour at the same temperature) then a solution of the cyclic chlorophosphite **15** (prepared according to literature procedure [47] from racemic 1,1'-*bis*-2-naphtol and PCl_3) in THF was added drop wise at -78 °C then stirred at room temperature overnight.

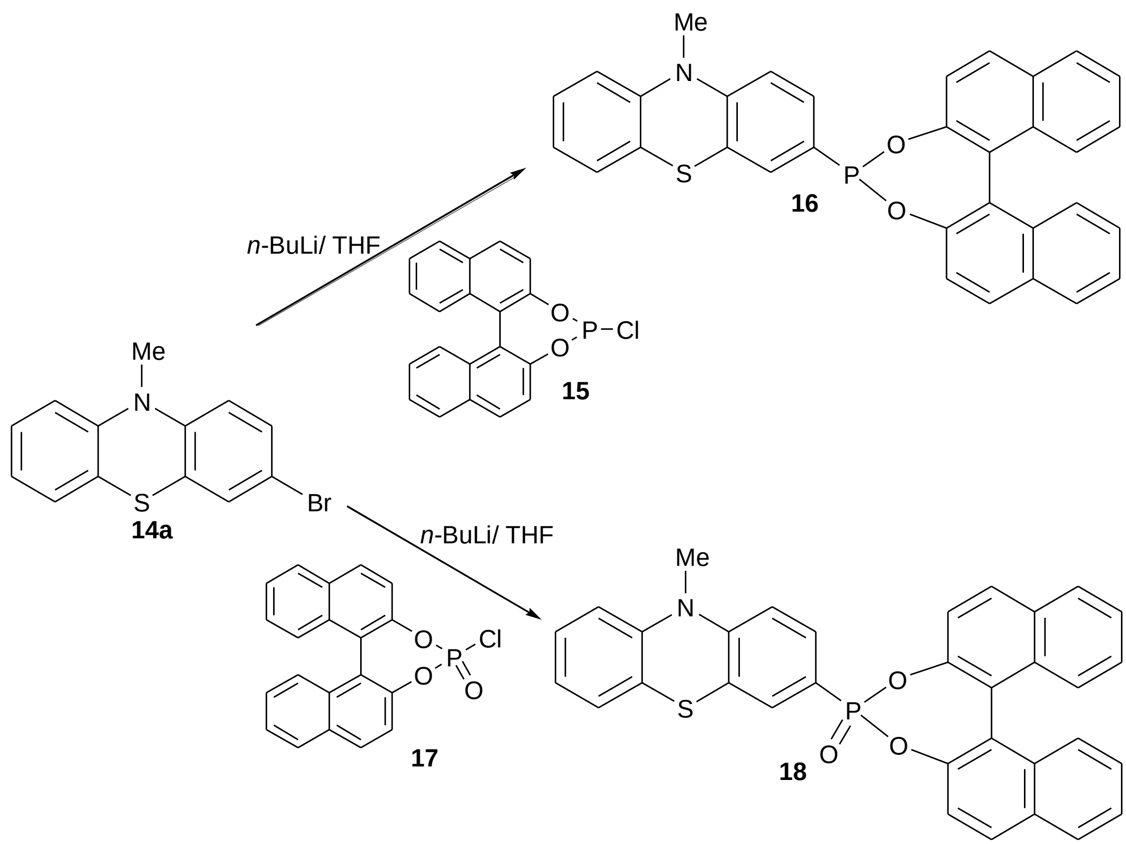

Scheme III.4. Synthesis of phenothiazinyl-phosphites **16** and **18**

The ^{31}P-NMR spectrum of compound **16** shows one signal at -19.1 ppm compared to 177.8 ppm in compound **15**, but the ^{1}H-NMR spectrum is not conclusive as all attempts to purify this compound have failed. In the mass spectrum of the isolated compound the *m/z* = 527 peak can be observed, confirming the formation of hypophosphite **16**, which is obtained as a white powder. Other observed peaks are *m/z*=512 (corresponding to the loss of the methyl group), *m/z*=315 (corresponding to the $C_{20}H_{12}O_2P^{\cdot+}$ from the bis-naphtol moiety), but also *m/z*=543, corresponding to the oxidation of P(III) to P(V).

Taking into account the sensitivity of P(III) towards oxidation, the P(V) analogue was synthesized (compound **18**) hoping to a more successful purification. Unfortunately, compound

18 could not be purified enough either. It was prepared following the same synthetic pathway: the same method was applied for the synthesis of **17**, starting from racemic 1,1'-bis-2-naphtol and $POCl_3$ and the same steps were followed for lithiation and electrophilic substitution. The ^{31}P-NMR spectrum of compound **18** shows one signal at 1.2 ppm, in the same range where similar compounds appear [48]. The starting chlorophosphite **17** has the P chemical shift 13.9 ppm. In the mass spectrum of compound **18** the molecular peak *m/z*=543 can be observed along with other characteristic peaks, such as *m/z*=528 (corresponding to the loss of the methyl group) or *m/z*=268 (base peak, corresponding to $C_{20}H_{12}O^+$ from the bis-naphtol moiety). Phosphite **18** is an orange powder, insoluble in chloroform, methanol, tetrahydrofurane, pentane or toluene, being slightly soluble in DMSO.

III.3.2. Synthesis of phenothiazinyl-phosphines

The new diphenylphosphin-phenothiazines **22**, **23a**, **23b** and **24** were prepared by lithiation-electrophilic substitution. In order to introduce the phosphinic moiety in positions 1 or 3 of the phenothiazinyl ring, 1-bromo-10-methyl-phenothiazine and 3-bromo-10-alkyl-phenothiazine (methyl or ethyl) respectively were used for lithiation with *n*-BuLi in diethylether at -78 °C (slightly modified procedure of Katritzky *et al* [49]). If there is no substituent on the phenyl rings of 10-alkyl-phenothiazine lithiation occurs in position 4. The best results were obtained using *t*-BuLi in THF at 0 °C in the presence of TMEDA, a diamine with chelating properties. The lithio-derivatives were then reacted with diphenylchlorophosphine (**Scheme III.5.**). A similar procedure for lithiation was previously described [46]. The yields for obtaining these ligands are moderate, due to the difficulty of selective monofunctionalisation of a symmetrical backbone (*e.g*. concomitant formation of the corresponding bisphosphines).

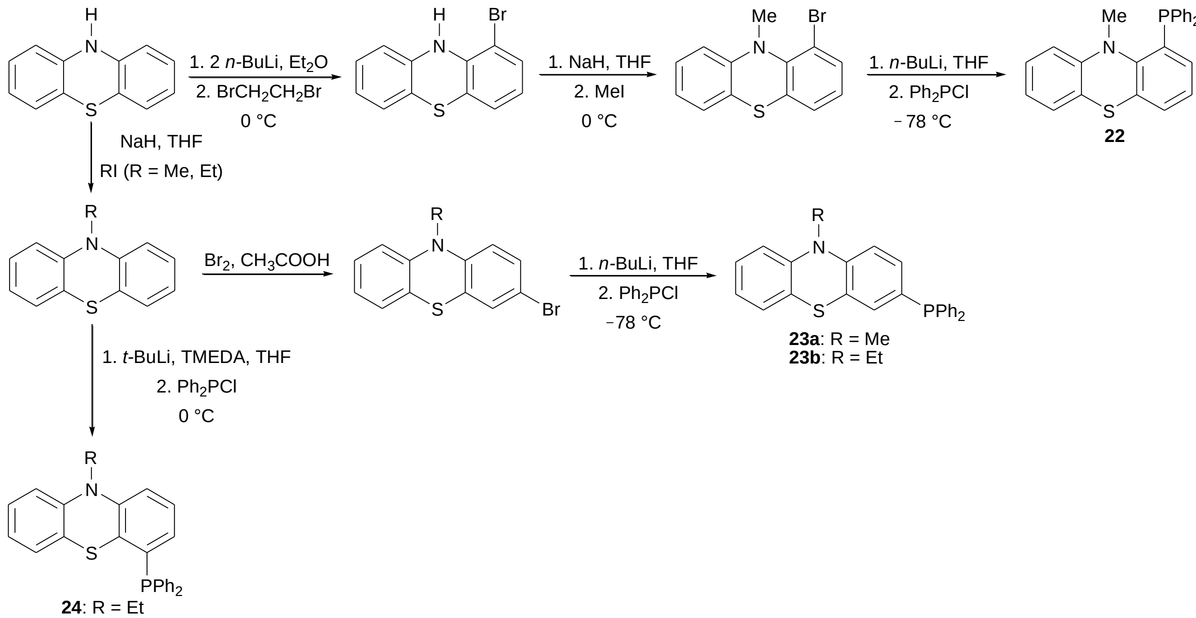

Scheme III.5. Synthesis of phenothiazinyl-phosphine ligands **22**, **23a**, **23b** and **24**

The ^{31}P-NMR spectrum of compound **22** shows one signal at δ = -8.9 ppm, for compounds **23a** and **23b** at -6.9 and -7.0 ppm respectively, while compound **24** has the most shielded P atom, at -13.2 ppm. In case of compound **22**, in the ^{13}C-NMR spectrum, besides the usual coupling constants, coupling between the P and the C^{11} atom can be observed, the value of the coupling constant being 17 Hz. The C-P coupling constants have similar values to other phosphorus-aryl containing compounds [50]. Compounds **23a** and **23b** have similar spectra because of their similar structures. In all of these cases, the observed $^1J_{PC}$ and $^3J_{PC}$ have smaller values (10.2 and 7.5 Hz respectively) compared to $^2J_{PC}$, which is bigger (19.9 or 22.5 Hz). For example, some observed coupling constants in compound **23b** are $^2J_{PC}$ = 19.3 Hz for the *orto*-C atoms, $^1J_{PC}$ = 10.4 Hz for the *ipso*-C atoms (C^{13}) and $^3J_{PC}$ = 6.9 Hz for the *meta*-C atoms of the phenyl rings. Similar values were observed in case of compound **24**: $^2J_{PC}$ = 19.9 Hz for the *orto*-C atoms, $^1J_{PC}$ = 10.2 Hz for the *ipso*-C atoms or $^3J_{PC}$ = 7.2 Hz for the *meta*-C atoms of the phenyl rings.

The electronic properties of phenothiazinyl-phosphines **22**, **23b** and **24** were investigated by absorption/emission UV-vis spectroscopy and cyclic voltammetry. UV absorption and emission data of dilute solutions are shown in **Table III.2.** UV absorption spectra of the dilute solutions are shown in **Fig. III.5**.

Table III.2. Absorption and emission data of compounds **22**, **23b** and **24**

Compound	Absorption $\lambda_{max.abs}$ (nm)	Emission $\lambda_{max.em}$(nm)	Quantum yield Φ (%)	Stokes shift (cm^{-1})
22	253, <u>313</u>	464	0.5	10397
23b	262, <u>311</u>	458	4.6	10320
24	252, <u>305</u>	456	0.5	10857

The concentrations of the solutions used for fluorescence measurements were: $5.1 \cdot 10^{-7}$ M for **22**, $2.1 \cdot 10^{-5}$ M for **23b** and **24**. The excitation wavelength was has been underlined. Quantum yields were calculated reported to perylene according to ref. [51].

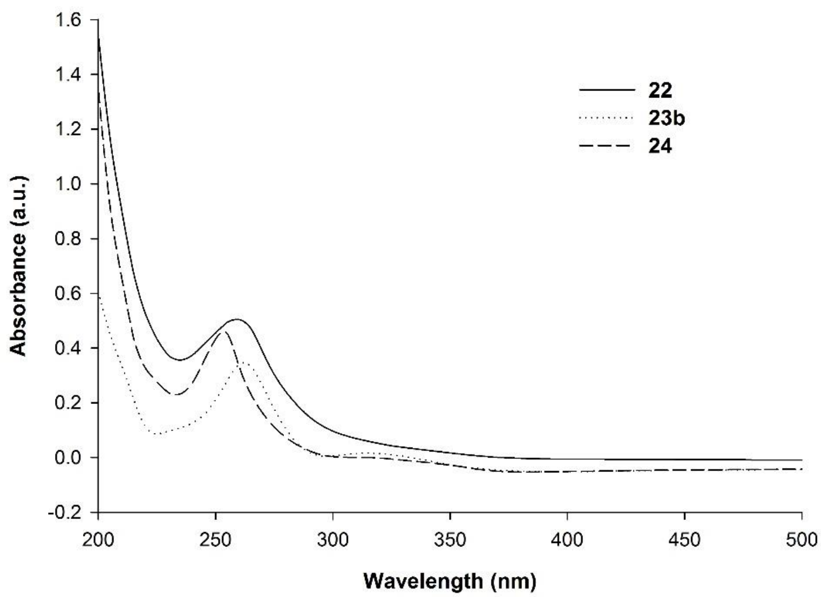

Fig. III.5. UV absorption spectra of the dilute acetonitrile solutions of regioisomers **22**, **23b** and **24** (c = $2.6 \cdot 10^{-5}$ M for **22**, 10^{-5} M for **23b** and $2.3 \cdot 10^{-5}$ M for **24**)

The fluorescence spectra of compounds **22**, **23b** and **24** are shown in **Figure III.7**. While compounds **22** and **24** had similar quantum yields of only 0.5%, for compound **23b** the calculated quantum yield was 4.6%, related to perylene standard. The calculated Stokes shifts are presented in **Table III.2**.

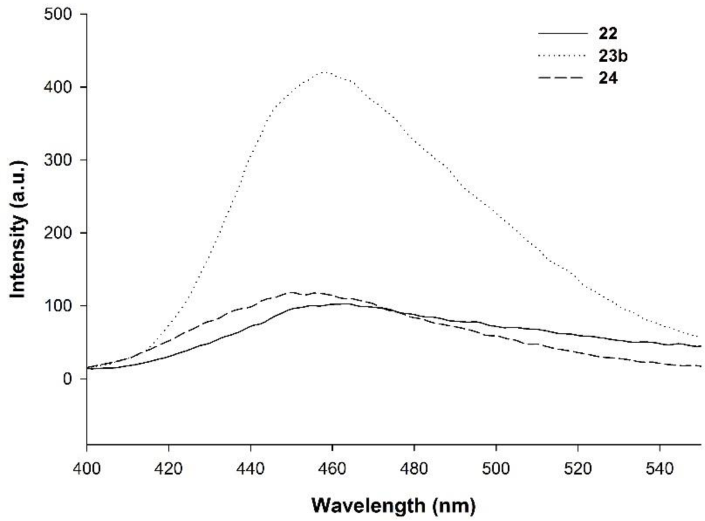

Fig. III.7. Fluorescence spectra of compounds **22**, **23b** and **24** (c = $5.1 \cdot 10^{-7}$ M for **22**, $2.1 \cdot 10^{-7}$ M for **23b** and $9.2 \cdot 10^{-7}$ M for **24**; λ_{ex} = 313 nm for **22**, 311 nm for **23b** and 305 nm for **24**)

To provide more details on the different behavior of these ligands, DFT calculations (B3LYP/6-311G(2d,2p)) were performed on the ground states as well as on the excited states of **22**, **23b** and **24**. In the ground state, **22**, **23b** and **24** display typical phenothiazine geometries, folded against the N-S axes.

Cyclic voltammetry (CV) experiments were carried out in dichloromethane, using ferrocene/ferrocenium (Fc/Fc^+) as internal standard, with scanning in the anodic (up to 1.8V) and cathodic (up to -0.2 V) region. The cyclic voltammograms are shown in **Figure III.9** and the electrochemical data are presented in **Table III.4.** In case of compound **22**, only one oxidation potential was observed (0.976 V) and was attributed to the phenothiazine moiety. In case of compounds **23b** and **24**, the first oxidation potential belongs to phenothiazine moiety and is qvasireversible for these compounds while the second oxidation potential for compound **23b** (1.109 V) and second and third oxidation potentials (1.112 V and 1.446 V, respectively) for compound **24** are generated by phosphorus oxidation and the processes are irreversible.

Table III.4. Cyclic voltammetry data E (V) for compounds **22**, **23b** and **24**

Compound	$E_{1/2(1)}$	$E_{1/2(2)}$	$E_{1/2(3)}$
22	0.976	-	-
23b	0.827	1.109	-
24	0.825	1.112	1.446

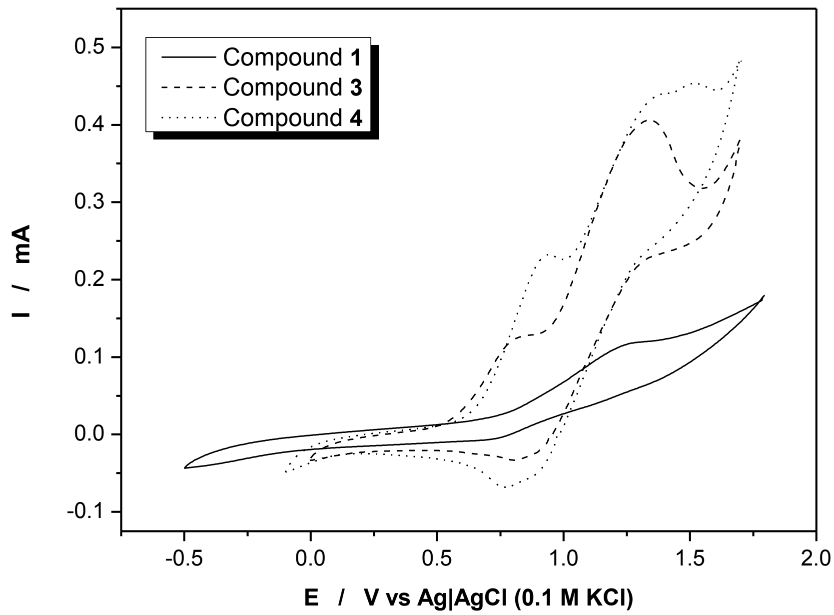

Fig. III.9. Cyclic voltammogram of compounds **22, 23b** and **24** recorded in a solution of 0.1 M $TBAPF_6$ (tetrabutylammoniumhexafluorophosphate) in CH_2Cl_2 as a supporting electrolyte; starting potential: -2.0 V vs. SCE (Saturated Calomel Electrode), scan rate: v = 50 mV/s. The reference electrode consisted of a silver wire (diameter ~ 1 mm, length ~ 10 cm) coated with AgCl and dipped into a 1 M KCl solution. A glassy carbon electrode (3 mm) was used as the working electrode and a Pt wire as the counter electrode.

III.3.3. Transition metal complexes

In order to study the coordination mode of the synthesized ligands, they were reacted with [MCl_2(cod)] (M=Pd, Pt) in dichloromethane. In case of ligand **22**, the proposed structures are presented in **Scheme III.6**. The chemical shift of the phosphorus atom in ^{31}P-NMR (42.9 ppm) is shifted to lower fields compared to the free ligand by *ca*. 51.8 ppm.

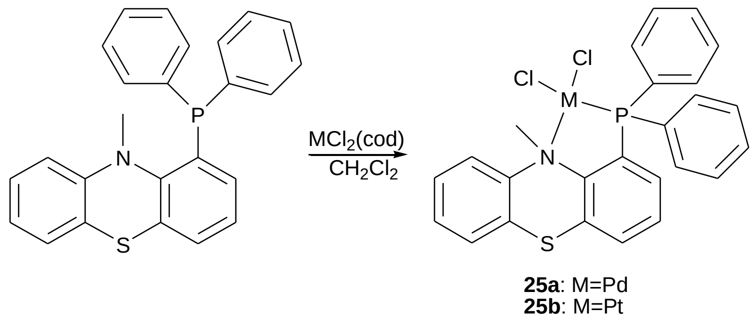

Scheme III.6. Synthesis of complexes **25a** and **25b**

The proposed structure was confirmed by X-ray diffraction measurement on a single crystal of complex **25a**. Compound **22** acts as a bidentate ligand coordinating to the Pd centre with its two heteroatoms, N and P. Complex **25a** crystallizes in $P\bar{1}$ space group with 2 molecules in the unit cell. The units contain a dichloromethane solvate molecule. The solid state structure of complex **25a** is presented in **Fig. III.10.** while selected bond lengths and angles can be found in **Table III.4**. The palladium atom is situated in a slightly distorted square-planar geometry.

Table III.4. Selected bond lengths (Å) and angles (°) for **25a**

Pd(1)-N(1)	2.161(1)	N(1)-Pd(1)-P(1)	86.18(4)
Pd(1)-P(1)	2.1829(5)	P(1)-Pd(1)-Cl(2)	86.99(2)
Pd(1)-Cl(2)	2.2936(4)	N(1)-Pd(1)-Cl(1)	94.68(4)
Pd(1)-Cl(1)	2.3925(5)	P(1)-Pd(1)-Cl(1)	176.74(2)
S(1)-C(8)	1.751(3)	Cl(2)-Pd(1)-Cl(1)	92.44(2)
P(1)-C(14)	1.797(2)	C(12)-P(1)-C(14)	105.52(9)
P(1)-C(20)	1.804(2)	C(14)-P(1)-C(20)	108.01(9)
P(1)-C(12)	1.7962(2)	C(12)-P(1)-Pd(1)	102.51(7)
N(1)-C(1)	1.473(2)	C(14)-P(1)-Pd(1)	119.60(6)
N(1)-C(7)	1.479(2)	C(20)-P(1)-Pd(1)	113.02(7)
N(1)-C(13)	1.519(2)	C(1)-N(1)-Pd(1)	117.70(1)
		C(7)-N(1)-Pd(1)	112.50(1)
		C(13)-N(1)-Pd(1)	98.90(1)

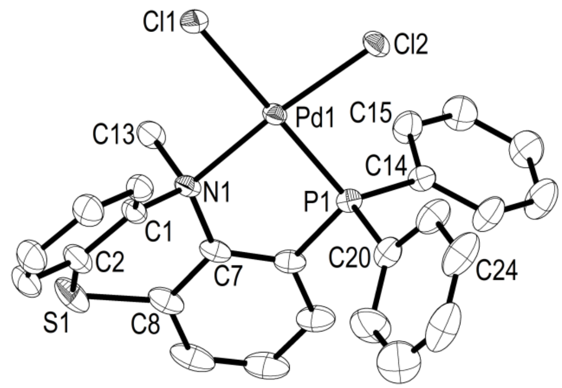

Fig. III.10. Solid state molecular structure of complex **25a**.

When the reaction between ligand **22** and [$PtCl_2$(cod)] was performed, next to the expected platinum complex **25b** another complex (**25c**) is obtained. The two complexes could not be separated and the assumptions regarding their structures were made based on the NMR and ESI-MS spectra of the mixture. Two signals with the appropriate platinum satellites can be observed in the ^{31}P-NMR spectrum, at 14.8 ppm ($^1J_{PtP}$ = 3808 Hz) and 14.9 ppm ($^1J_{PtP}$ = 2714 Hz). We assigned the first signal as belonging to complex **25b** and we proposed a dimeric structure for complex **25c**, as can be seen in **Fig. III.11**. The two complexes are in a 1:1.4 ratio (**25b**:**25c**) in solution. The ESI-MS spectrum shows a peak corresponding to the [M-Cl]$^+$ fragment at *m/z*=1025.15.

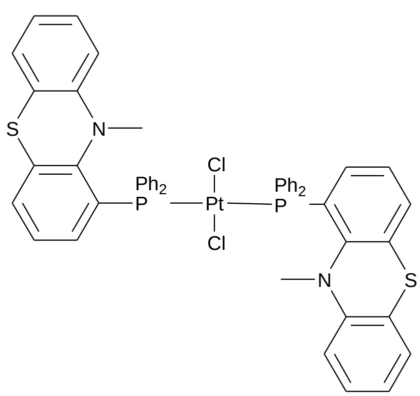

Fig. III.11. Proposed structure for dimer resulted in the reaction of ligand **22** with [$PtCl_2$(cod)]

An experiment in which ligands **23a** and **23b** were reacted with [$PdCl_2$(cod)] and [$PtCl_2$(cod)] (cod = 1,5-cyclooctadiene) in a 2:1 molar ratio was performed. The change in the colour of the solutions and the ^{31}P-NMR spectra of the reaction mixtures confirmed coordination of ligands **23a** and **23b** to Pd or Pt. The proposed structures for the transition metal complexes are presented in **Scheme III.7.**

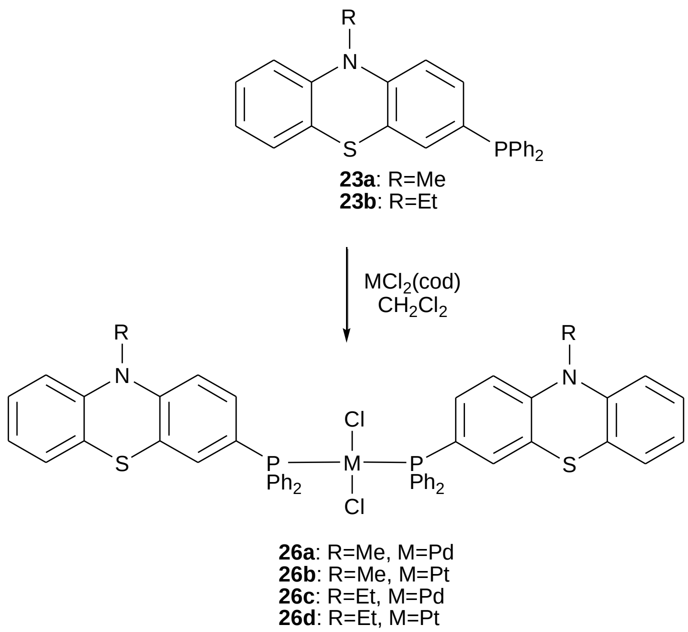

Scheme III.7. Reaction of ligands **23a** and **23b** with transition metals (M=Pd, Pt)

The P atom of the palladium complexes **26a** and **26c** are shifted to higher field (22.3 ppm in **26a**, 22.1 ppm in **26c**) compared to the free ligand (-6.9 ppm in **23a**, -7.0 ppm in **23b**). In the case of the platinum complexes **26b** and **26d** the phosphorus atom is also shifted to higher fields compared to the free ligand (13.2 ppm in **26b**, 13.0 ppm in **26d**), the $^{1}J_{PtP}$ coupling constants having similar values ($^{1}J_{PtP}$ = 3699 Hz in **26b**, $^{1}J_{PtP}$ = 3672 Hz in **26d**). The chemical shifts and coupling constants in the ^{1}H and ^{13}C-NMR spectra are similar in complexes **26a** and **26b** to **26c** and **26d** respectively.

Crystals of the palladium complex **26a** were obtained and the solid state structure could be determined by X-ray diffraction measurements (**Fig. III.13.**). Complex **26a** crystallizes in the triclinic $P\bar{1}$ space group with only one molecule in the unit cell.

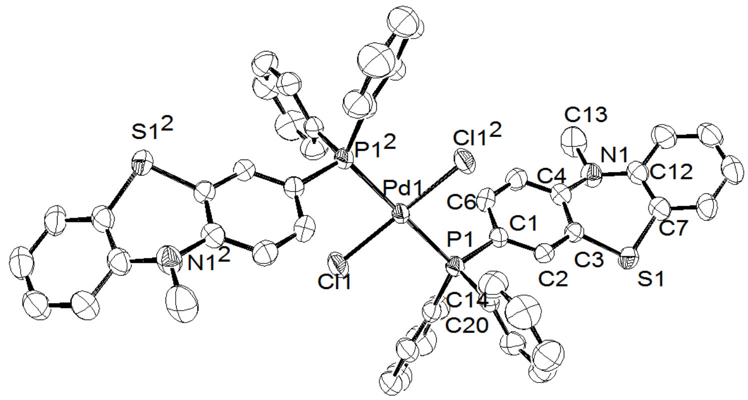

Fig. III.13. ORTEP drawing of **26a**.

On treating ligand **24** with [$PdCl_2$(cod)] and [$PtCl_2$(cod)] (cod = 1,5-cyclooctadiene) in a 1:1 molar ratio complexes **27a** and **27b** could be isolated (**Scheme III.8.**). Compound **27a** could be isolated like dark orange crystals while compound **27b** has a green-yellow colour.

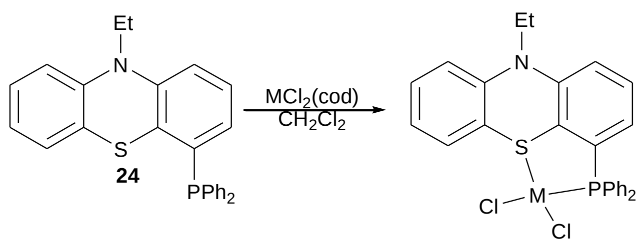

Scheme III.8. Synthesis of transition metal complexes of **24**

The chemical shifts of the P atoms in ^{31}P-NMR are shifted to lower field compared to the free ligand (δ = 59.5 ppm in **27a** and δ = 36.6 ppm in **27b** compared to the free ligand where the chemical shift of the P atom is -13.2 ppm). The observed coupling constant ($^{1}J_{PtP}$ = 3490 Hz) is strongly correlated with the Pt-P bond length.

Crystals suitable for X-ray diffraction measurements were obtained from dichloromethane. **27a** crystallizes as dark orange crystals while **27b** has yellow crystals. Both complexes crystallize in $P2_1$/n space group, in a monoclinic crystal system with 4 molecules in the unit cell. The molecular structures of **27a** is presented in **fig. III.14.a**. **27b** is isostructural to **27a**.

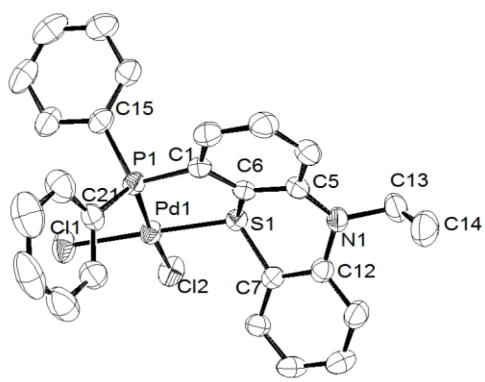

Fig. III.14.a. Molecular structure of complex **27a**.

The absorption and emission spectra of some of the synthesized complexes were recorded. The data are presented in **Table III.7.** and **Table III.8.** Compound **25a** has an UV absorption maximum at 228 nm. Compounds **26a** and **26c** exhibit similar behaviour, having their maximum absorption peak at 263 nm. A similar behaviour can be observed in the case of the platinum complexes **26b** and **26d** (267 and 268 nm, respectively). One additional peak can be observed in the case of the palladium complexes of the ligands compared to the platinum complexes of the same ligands.

Table III.7. UV absorption data for the transition metal complexes

Compound	λ (nm)	A (a.u.)	Concentration (M)
25a	228	0.7240	
	281	0.3463	$2.5\cdot10^{-6}$
	356	0.0470	
26a	227	0.5869	
	263	0.7060	10^{-5}
	335	0.2236	
	400	0.0953	
26c	229	0.5185	
	263	0.7253	10^{-5}
	336	0.2389	
	404	0.0963	
27a	228	0.5290	
	287	0.1913	$2\cdot10^{-5}$
	417	0.0298	
26b	234	0.4810	
	268	0.5775	10^{-5}
	318	0.1044	
26d	227	0.5339	
	267	0.8257	10^{-5}
	318	0.1649	

27b	229 327	0.6722 0.0675	$2\cdot10^{-5}$

Among the transition metal complexes, the highest quantum yield was observed for complex **26a** (4.8%). *Bis*-(*N*-ethyl-3-diphenylphosphin-phenothizinyl) palladium or platinum complexes had lower quantum yields than their methyl analogues, disregarding the transitional metal. The lowest quantum yield was observed for the palladium complex of ligand **24**; its platinum complex did not exhibit fluorescence. In the case of the transition metal complexes, quantum yields were calculated reported to naphthalene.

Table III.8. Emission data for the transition metal complexes

Compound	λ_{ex} (nm)	λ_{em} (nm)	Stokes shift (cm^{-1})	Φ
25a	281	375	8920.52	0.009
26a	263	375	11356.14	0.048
26c	263	368	10848.90	0.028
27a	287	370	7816.18	0.0025
26b	268	371	10359.26	0.035
26d	267	366	10130.78	0.029
27b	Has no fluorescence			

III.3.4. Catalytic activity of phenothiazinyl-phosphines in hydrogenation reactions

Our experiments involvedα,β-unsaturated ketones having one or two electron-rich substituents like phenothiazine in compounds **28a**-**e**. The catalyst generated in situ from palladium acetate and hemilabile ligand **24** reduced the C-C double bond to yield ketones or both the C-C and C-O double bonds to yield alcohols (**Scheme III.9**). The yields of pure isolated compounds by column chromatography are presented in **Table III.7**.

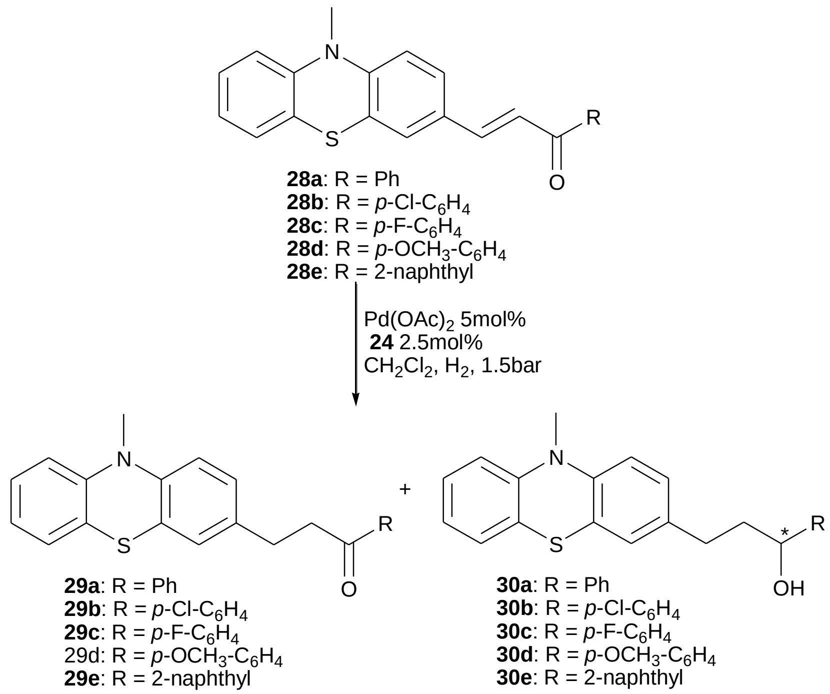

Scheme III.9. Reduction of C-C and C-O double bonds in chalcones

Table III.7. Yields of pure isolated compounds

Compound	Yield (%)	Compound	Yield (%)
29a	40	**30a**	40
29b	40	**30b**	40
29c	45	**30c**	40
29d	35	**30d**	30
29e	40	**30e**	40

After the hydrogenation process of α,β-unsaturated ketones **28a**-**e**, in the presence of the palladium complex of ligand **24**, two reduced compounds were isolated, the ketone generated by C-C double bond reduction and the alcohol generated by C-C and C-O double bonds reduction. The ratio between ketones **29a**-**e** and alcohols **30a**-**e** was almost 1:1 (**Table III.7**). If the α,β-unsaturated ketone **28a-e** contained one or two electron donor substituents a complete reduction to alcohol was impossible to achieve.

The catalyst was prepared by the *in situ* reaction of ligand **24** and palladium acetate in a mixture of dichloromethane: isopropanol = 1:1, the reaction being followed by ^{31}P-NMR spectroscopy. The catalytic cycle, proposed according to a similar example from the literature [56], is presented in **Scheme III.12**.

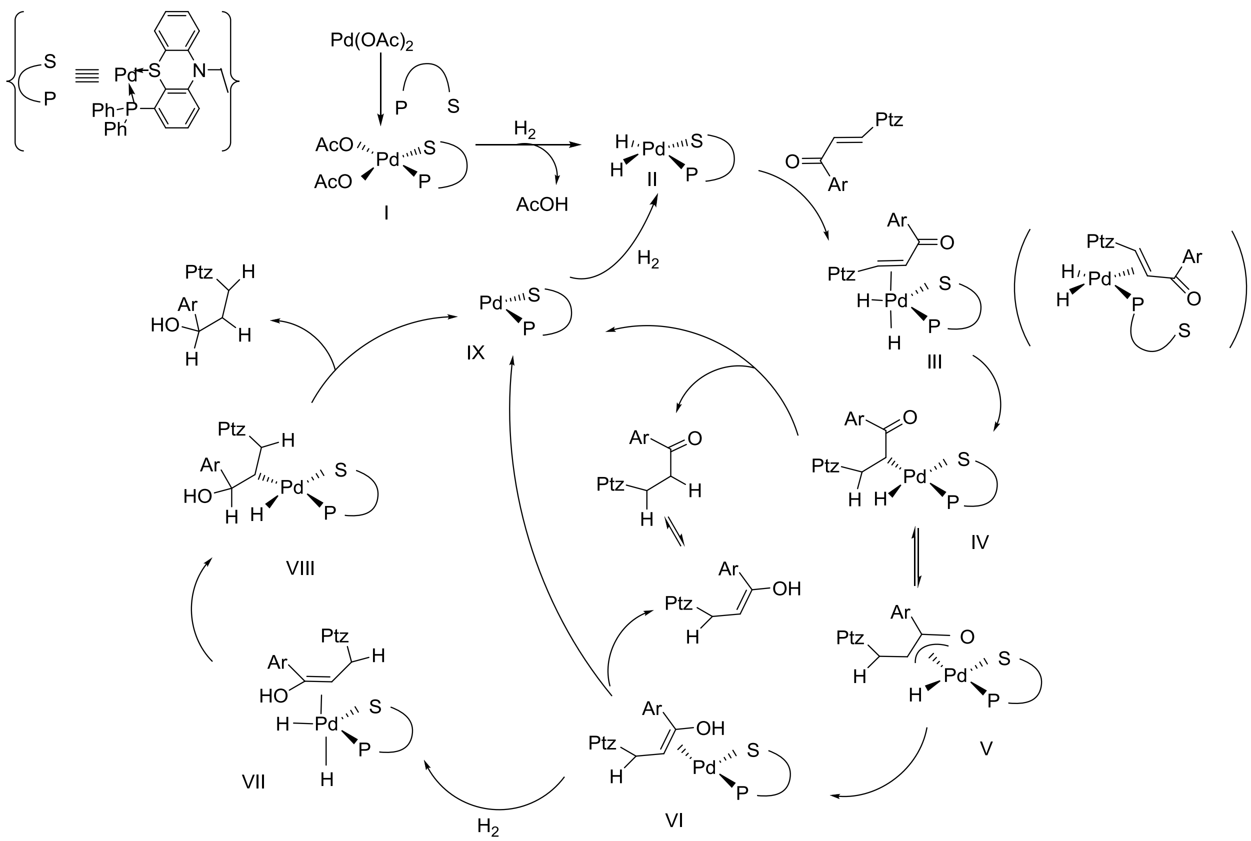

Scheme III.12. Proposed catalytic cycle for hydrogenation of α,β-unsaturated ketones

Steps of the catalytic cycle:

1. Ligand coordination to form complex **I**
2. Oxidative addition of hydrogen followed by reductive elimination of acetic acid to generate complex **II**
3. Coordination of the chalcone to the palladium centre thought C=C bond with the possible hemilabile ligand (S) decoordination from the metal centre
4. Migratory insertion (syn) of vinyl group in the metal hydride bond to generate complex **IV**
5. Reductive elimination (syn) of the saturated ketone and complex **IX**, which by hydrogen oxidative addition can yield complex **II**

The alcohol formation can be explaining by the following steps from the catalytic cycle:

6. Keto-enol tautomerization assisted by Pd and hemilabile ligand **24**, followed by migratory insertion and enone coordination to the **24**-Pd(0) complex
7. Oxidative addition of hydrogen (*cis*), generating an (enolate)**24**H_2Pd(II) species

8. Migratory insertion followed by reductive elimination yields the desired saturated alcohol and **24**-Pd(0) complex.

III.3.5. Biological activity of phenothiazinyl-phosphines and their transition metal complexes

The interaction of phenothiazinyl-phosphines **22**, **23b** and **24** and metal complexes **27a** and **27b** with DNA was investigated by electrophoresis (**Fig III.15**). Experiments indicate that phenothiazinyl-phosphines **22** and **23b** interact with DNA molecules and change their physical properties (**Fig. III.15a**, lanes 5-7; **Fig III.15b**, lanes 5 and 6), so that the modified DNA does not migrate during electrophoresis and can be observed in the start line. For phenothiazinyl-phosphine **24** the capacity to interact with DNA is diminished because of the steric hindrance of the phosphine moiety at low concentrations. Only at the maximum tested concentration of compound **24** (**Fig III.15b**, lane 13) some modified DNA does not migrate during electrophoresis.

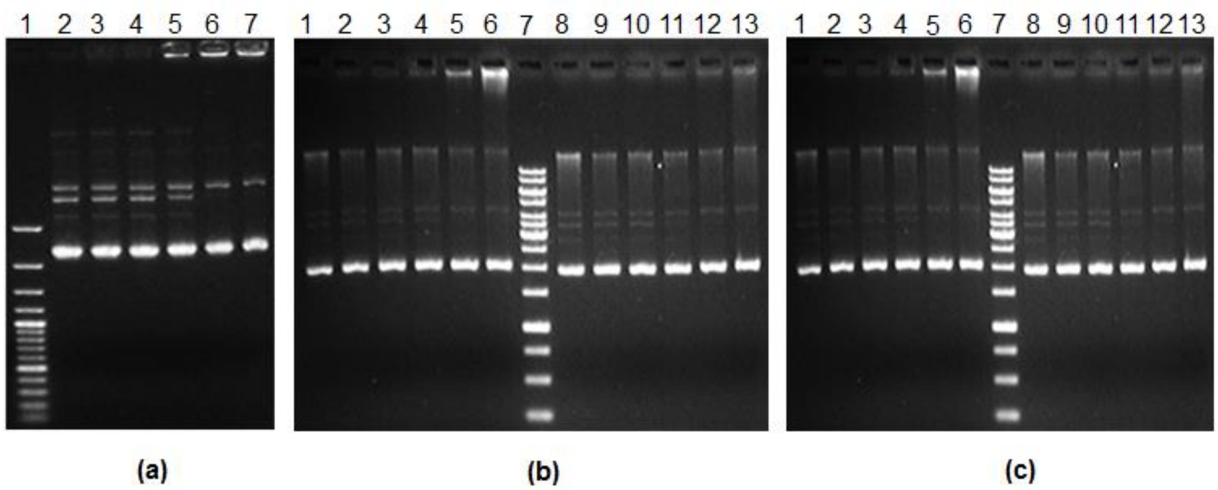

Fig III.15. Interaction of **22** (a), **23b, 24** (b), **27a** and **27b** (c) with plasmid DNA (pTZ57R). (a) Lane 1: GeneRuler 100bp Plus DNA ladder (Thermo Scientific); lane 2: closed circular plasmid DNA without complex to be tested; lanes 3-7: plasmid DNA with 0.5, 1, 2, 4 and 8 μl of **22**. (b) Lanes 1 and 8: closed circular plasmid DNA without complex to be tested; lanes 2-6: plasmid DNA with 0.5, 1, 2, 4 and 8 μl of **23b** respectively; lanes 9-13: plasmid DNA with 0.5, 1, 2, 4 and 8 μl of **24**; lane 7: GeneRuler 1 kb DNA ladder (Thermo Scientific). (c) Lanes 1 and 8: closed circular plasmid DNA without complex to be tested; lanes 2-6: plasmid DNA with 0.5, 1, 2, 4 and 8 μl of **27a** respectively; lanes 9-13: plasmid DNA with 0.5, 1, 2, 4 and 8 μl of **27b**; lane 7: GeneRuler 1 kb DNA ladder (Thermo Scientific).

The Pd and Pt complexes of phenothiazinyl-phosphine **24** are capable of interacting with DNA (**Fig III.15c** lines 2-6 and 10-13 respectively) generating molecular aggregates that in the electrophoresis experiment have a different migration capacity compared to that of the free DNA. For the identification of the exact type of interactions between the tested molecules and DNA further investigations are necessary.

III.3.5.2. Cytotoxicity of complexes 26b and 27b

The cytotoxicity of complexes **26b** and **27c** was tested on 3 cell lines: breast carcinoma, hepatocarcinoma and colorectal carcinoma. The platinum(II) complex **25b** could not be obtained in pure form, and complex **26d** is similar to its methyl analogue **26b**; therefore, these complexes were not tested.

The viability of all three cell lines decreased proportionally with the increase of the concentration of both compounds. The concentrations which reduced viability with 50% (IC_{50}) for compound **27b** were: 19.01 µg/ ml for the breast carcinoma (MCF7) cell line, 63.79 µg/ ml for the hepatocarcinoma (HepG2) cell line, and 74.49 µg/ ml for colorectal carcinoma (DLD1) cell line indicating that the breast carcinoma cell line was the most affected, while the the hepatocarcinoma and colorectal carcinoma cell lines required a significantly higher concentration of the compound to reduce their viability with 50%. For compound **26b**, the behaviour of all three cell lines was similar, and again breast carcinoma cell line was the most sensitive (IC_{50}= 49.56 µg/ ml), while colorectal and hepatocarcinomas behaved almost identically (IC_{50}DLD1= 51.40 µg/ ml, IC_{50}HepG2= 54.68 µg/ ml). The IC_{50} values were calculated using nonlinear regression and four-parameter sigmoidal curve fit, each point representing mean ± SEM (standard error of the mean) in three separate measurements.

III.3.6. Conclusions

2 new phenothiazinyl-phosphites **16** and **18** were prepared, but purification methods failed, the compounds being characterized only by ^{31}P-NMR and mass spectrometry.

Lithiation followed by electrophilic substitution reaction had different outcomes depending on the substrate. Diphenylphosphinic moiety was introduced in positions 1, 3 and 4 of the phenothiazine unit. By this method, 2 new phenothiazinyl-phosphines were prepared and characterized (**22** and **23b**). The synthesis of **23a** [45] and **24** [46] has already been reported but a slightly different procedure was used. The electronic properties of phenothiazinyl-phosphines

22, **23b** and **24** were investigated by absorption/emission UV-vis spectroscopy, cyclic voltammetry and DFT calculations.

Transition metal complexes of the synthesized ligands were prepared and characterized. The formation of complex **27a** [46] was observed by ^{31}P-NMR measurements but the palladium complex was not isolated. In this work, complex **27a** was crystallised and its molecular structure was measured by X-ray diffraction measurements. In addition, the isostructural platinum complex **27b** of the same ligand (**24**) was prepared and characterized. Palladium complexes **25a**, **26a** and **26c** and platinum complexes **25b**, **26b** and **26d** were also prepared and characterised. The UV-vis absorption and emission spectroscopic properties of complexes **25a**, **26a**-**d** and **27a**-**b** were investigated. The catalytic activity of ligands **22**, **23a** and **24** in the hydrogenation reaction of α,β-unsaturated ketones was evaluated.

The interaction of ligands **22**, **23b** and **24** and complexes **27a** and **27b** with plasmid DNA was studied. In addition, the cytotoxic effect of complexes **26b** and **27b** towards human breast adenocarcinoma, hepatocyte carcinoma and colorectal adenocarcinoma was also studied.

The quantum yield of the phosphanyl-substituted phenothiazines **22**, **23b** and **24** was observed to decrease upon coordination to Pd(II) and Pt(II). A higher DNA binding capacity was observed in case of compound **23b** compared to compounds **22** and **24**. Complexes **27a** and **27b** also bind to DNA, generating molecular aggregates. Compound **27b** showed better cytotoxic activity against breast carcinoma, but had a lower effect on hepatocarcinoma and colorectal carcinoma cell lines than compound **26b**.

References

[1] C. Lauth, *Ber. Deut. Chem. Ges*., *9* (**1913**) 1035.

[2] A. Bernsthsen, *Ber. Deut. Chem. Ges*., *45* (**1912**) 2012.

[3] G.M. Findlat, *Recent Advances in Chemotherapy*, 3rd edition ed., **1950**.

[4] J. Cymerman-Craig, W.P. Rogers, M.E. Tate, *Aust. J. Chem*., *9* (**1956**) 397.

[5] C. Bodea, I.A. Silberg, *Adv. Heterocycl. Chem*., *9* (**1968**) 321.

[6] H.M.L. Gordon, M.J. Lipson, *Connc. Sci. Ind. Res*., *13* (**1940**) 173.

[7] N. Griffon, C. Pilon, F. Santel, J.C. Schwartz, P. Sokoloff, *J. Neural. Trans*., *103* (**1996**) 1163.

[8] Z. Eckstein, T. Urbanski, *Adv. Heterocycl. Chem*., *23* (**1978**) 1.

[9] M. Ionescu, H. Mantsch, *Adv. Heterocycl. Chem*., *8* (**1967**) 83.

[10] W.E.J. Jr., P. Chen, T.J. Meyer, *J. Am. Chem. Soc*., *114* (**1992**) 387.

[11] T. Okamoto, M. Kuratsu, M. Kozaki, K. Hirotsu, A. Ichimura, T. Matsushita, K. Okada, *Org. Lett*., *6* (**2004**) 3493.

[12] H. Oka, *J. Mater. Chem*., *18* (**2008**) 1927.

[13] M. Sailer, A.W. Franz, T.J.J. Müller, *Chem. Eur. J*., *14* (**2008**) 2602.

[14] A.W. Franz, L.N. Popa, F. Rominger, T.J.J. Müller, *Org. Biomol. Chem*., *7* (**2009**) 469.

[15] A.W. Franz, L.N. Popa, T.J.J. Müller, *Tetrahedron Lett*., *49* (**2008**) 3300.

[16] J. Strauss, J. Daub, *J. Adv. Mater*., *14* (**2002**) 1652.

[17] T. Meyer, D. Ogermann, A. Pankrath, K. Kleinermanns, T.J.J. Müller, *J. Org. Chem*., *77* (**2012**) 3704.

[18] J.C. Jeffrey, T.B. Rauchfuss, *Inorg. Chem*., *18* (**1979**) 2658.

[19] J.A. Davies, F.R. Hartley, *Chem. Rev*., *81* (**1981**) 79.

[20] F.R. Knight, A.L. Fuller, A.M.Z. Slawin, J.D. Woollins, *Polyhedron*, *29* (**2010**) 1956.

[21] S. Kudis, G. Helmcken, *Angew. Chem., Int. Ed*. , *37* (**1998**) 3047.

[22] K. Yonehara, T. Hashizume, K. Mori, K. Ohe, S. Uemura, *Chem. Commun*., (**1999**) 415

[23] S. Hillebrand, J. Bruckmann, C. Krüger, M.W. Haenel, *Tetrahedron Lett*, *36* (**1995**) 75.

[24] M. Kranenburg, Y.E.M.v.d. Burgt, P.C.J. Kamer, P.W.N.M. van Leeuwen, *Organometallics*, *14* (**1995**) 3081.

[25] L.A. van der Veen, M.D.K. Boele, F.R. Bregman, P.C.J. Kamer, P.W.N.M. van Leeuwen, K. Goubitz, J. Fraanje, H. Schenk, C. Bo, *J. Am. Chem. Soc*., *120* (**1998**) 11616

[26] P. Dierkes, S.Ramdeehul, L. Barloy, A.D. Cian, J. Fischer, P.C.J. Kamer, P.W.N.M. van Leeuwen, J.A. Osborn, *Angew. Chem. Int. Ed*., *37* (**1998**) 3116.

[27] M.A. Zuideveld, B.H.G. Swennenhuis, M.D.K. Boele, Y. Guari, G.P.F. van Strijdonck, J.N.H. Reek, P.C.J. Kamer, K. Goubitz, J. Fraanje, M. Lutz, A.L. Spek, P.W.N.M. van Leeuwen, *J. Chem. Soc., Dalton Trans*., (**2002**) 2308.

[28] M.J.-L. Tschan, E.J. Garcia-Suàrez, Z. Freixa, H. Launay, H. Hagen, J. Benet-Buchholz, P.W.N.M. van Leeuwen, *J. Am. Chem. Soc*., *132* (**2010**) 6463.

[29] M.J.-L. Tschan, J.M. Lopez-Valbuena, Z. Freixa, H. Launay, H. Hagen, J. Benet-Buchholz, P.W.N.M. van Leeuwen, *Organometallics*, *30* (**2011**) 792.

[30] M.J.-L.Tschan, H. Launay, H. Hagen, J. Benet-Buchholz, P.W.N.M. van Leeuwen, *Chem. Eur. J.*, *17* (**2011**) 8922.

[31] M.W. Haenel, D. Jakubik, C. Krüger, P. Betz, *Chem. Ber*., *124* (**1991**) 333.

[32] M.W. Haenel, D. Jakubik, E. Rothenberger, G. Schroth, *Chem. Ber*., *124* (**1991**) 1705.

[33] M.W. Haenel, H. Fieseler, D. Jakubik, B. Gabor, R. Goddard, C. Krüger, *Tetrahedron Lett.*, *34* (**1993**) 2107.

[34] J.S. Nowick, P. Ballester, F. Ebmeyer, J.Rebeck Jr., *J. Am. Chem. Soc*., *112* (**1990**) 8902.

[35] L.A.v.d. Veen, P.H. Keeven, G.C. Schoemaker, J.N.H. Reek, P.C.J. Kamer, P.W.N.M. van Leeuwen, M. Lutz, A.L. Spek, *Organomet*., *19* (**2000**) 872.

[36] C.P. Casey, G.T. Whiteker, *Isr. J. Chem*., *30* (**1990**) 299.

[37] P.C.J. Kamer, P.W.N.M. van Leewen, J.N.H. Reek, *Acc. Chem. Res*., *34* (**2001**) 895.

[38] C.P. Casey, G.T. Whiteker, M.G. Melville, L.M. Petrovich, J.A.G. Jr., D.R. Powell, *J. Am. Chem. Soc*., *114* (**1992**) 5535.

[39] A.E.W. Ledger, P.A. Slatford, J.P. Lowe, M.F. Mahon, M.K. Whittlesey, J.M.J. Williams, *Dalton Trans*., (**2009**) 716.

[40] W.R. Moser, C.J. Papile, D.A. Brannon, R.A. Duwell, S.J. Weininger, *J. Mol. Catal*., *41* (**1987**) 271.

[41] J.D. Unruh, J.R. Christenson, *J. Mol. Catal*., *14* (**1982**) 19.

[42] D.J.H. Emslie, J.M. Blackwell, J.F. Britten, L.E. Harrington, *Organomet*., *25* (**2006**) 2412.

[43] D.J.H. Emslie, B.E. Cowie, S.R. Oakley, N.L. Huk, H.A. Jenkins, L.E. Harrington, J.F. Britten, *Dalton Trans*., *41* (**2012**) 3523.

[44] S.P. Ivonin, S.D. Kopteva, V.N. Serdyuk, A.A. Tolmachev, A.M. Pinchuk, *Heteroatom Chem*., *12* (**2001**) 652.

[45] T. Lovasz, E. Gal, L. Gaina, I. Sas, C. Cristea, L. Silaghi-Dumitrescu, *Studia UBB*. *Chemia*, *LV* (**2010**) 249.

[46] T. Lovasz, E. Gal, C. Cristea, L. Silaghi-Dumitrescu, *Studia UBB. Chemia, LVI* (**2011**) 191.

[47] K.C. Kumara Swamy, S. Kumaraswamy, K. Senthil Kumar, C. Muthiah, *Tetrahedron Lett*, *46* (**2005**).

[48] O. Kuhl, Phosphorus-31 NMR Spectroscopy. *A Concise Introduction for the Synthetic Organic and Organometallic Chemist*, Springer, Berlin, **2008**.

[49] A.R. Katritzky, H.Y. He, Q. Long, X. Cui, J. Level, A.L. Wilcox, *Arkivoc, iii* (**2000**) 240.

[50] A. Hildebrand, I. Sárosi, P. Lönnecke, L. Silaghi-Dumitrescu, M.B. Sárosi, I. Silaghi-Dumitrescu, E. Hey-Hawkins, *Dalton Trans*., *41* (**2012**) 7729.

[51] J.R. Albani, *Principles and Applications of Fluorescence Spectroscopy*, Blackwell Publishing, **2007**.

[52] K.M.M. MacKay, R.A., W. Henderson, *Introduction to Modern Inorganic Chemistry*, Cheltenham, United Kingdom, **2002**.

[53] P.G. Waddell, A.M.Z. Slawin, J.D. Woollins, *Dalton Trans*., *39* (**2010**) 8620.

[54] C.R. Hilliard, N. Bhuvanesh, J.A. Gladysz, J. Blumel, *Dalton Trans*., *41* (**2012**).

[55] R.J. Coyle, Y.L. Slovokhotov, M.Y. Antipin, V.V. Grushin, *Polyhedron*, *17* (**1998**) 3059.

[56] C. Amatore, A. Jutand, F. Khalil, *Arkivoc, iv* (**2006**) 38.

[57] A. Jaszczyszyn, K. Gasiorowski, P. Swiatek, W. Malinka, K. Cieslik-Boczula, J. Petrus, B. Czarnik-Matusewicz, *Pharmacol. Reports*, *64* (**2012**) 16.

[58] S.E. Kidd, T.W. Hambley, A. Hever, M.J. Nelson, J. Molnar, *J. Inorg. Biochem*., *62* (**1996**) 171.

[59] A. Hallberg, A.R. Martin, *Synthetic Commun.*, *13* (**1983**) 467.

[60] S. Ebdrup, *Synthesis*, (**1998**) 1107.

[61] D. Drew, J.R. Doyle, *Inorg. Synth*., *28* (**1990**) 346.

[62] CrysAlis Pro: Data collection and data reduction software package.

[63] SHELX: G. M. Sheldrick, *Acta Cryst.*, *A64* (**2008**), 112.

[64] C.K. Johnson, Report ORNL-5138, Oak Ridge National Laboratory, Oak Ridge, TN, **1976**.

[65] L.J. Farrugia, *Appl. Crystallogr*., *30* (**1997**) 565.

[66] *Gaussian 09*, Revision C.01, M. J. Frisch, G. W. Trucks, H. B. Schlegel, G. E. Scuseria, M. A. Robb, J. R. Cheeseman, G. Scalmani, V. Barone, B. Mennucci, G. A. Petersson, H. Nakatsuji, M. Caricato, X. Li, H. P. Hratchian, A. F. Izmaylov, J. Bloino, G. Zheng, J. L. Sonnenberg, M. Hada, M. Ehara, K. Toyota, R. Fukuda, J. Hasegawa, M. Ishida, T. Nakajima, Y. Honda, O. Kitao, H. Nakai, T. Vreven, J. A. J. Montgomery, J. E. Peralta, F. Ogliaro, M. Bearpark, J. J. Heyd, E. Brothers, K. N. Kudin, V. N. Staroverov, T. Keith, R. Kobayashi, J. Normand, K. Raghavachari, A. Rendell, J. C. Burant, S. S. Iyengar, J. Tomasi, M. Cossi, N. Rega, J. M. Millam, M. Klene, J. E. Knox, J. B. Cross, V. Bakken, C. Adamo, J. Jaramillo, R. Gomperts, R. E. Stratmann, O. Yazyev, A. J. Austin, R. Cammi, C. Pomelli, J. W. Ochterski, R. L. Martin, K. Morokuma, V. G. Zakrzewski, G. A. Voth, P. Salvador, J. J. Dannenberg, S. Dapprich, A. D. Daniels, O. Farkas, J. B. Foresman, J. V. Ortiz, J. Cioslowski and D. J. Fox, *Gaussian, Inc.,* Wallingford CT, **2009**.

[67] F.M. Ausubel, R. Brent, R.E. Kingston, D.M. Moore, J.G. Seidman, J.A. Smith, K. Struhl, *Short Protocols in Molecular Biology*, 5th ed., Wiley, New York, **2002**.

IV. Palladium complexes of N-alkyl-phenothiazines

IV.1. Introduction

Not only phenothiazine or its N-alkyl derivatives are known to be biologically active compounds, but also metal-phenothiazine-complexes. Although many transition metal-phenothiazine complexes have been synthesized and characterized, reports of their crystal structure are relatively limited [2-8]. This chapter presents the synthesis and characterization of *N*-alkyl-phenothiazine palladium complexes.

IV.2. Literature overview

Geary *et al.* [13] reported the X-ray structure of a unique palladium complex, the first crystallographic evidence for a coordinated phenothiazine drug. The complex was synthesized by the reaction of promethazine (10-[2(dimethylamino)propyl]phenothiazine) with potassium tetrachloropalladate in a 1:1 molar ratio and was considered a zwitterion with the nitrogen in the side chain being protonated and the ring sulfur coordinated to $PdCl_3^-$.

IV.3. Original contributions

IV.3.1. Synthesis and X-ray crystal structure of palladium complexes of *N*-alkyl-phenothiazines

Due to the relatively high electronegativity of the heterocyclic nitrogen atom, *N*-substitued phenothiazines **20a**-**c** could be prepared through electrofilic substitution reaction, according to literature procedures [16-18].

The palladium(II) complexes of *N*-substitued phenothiazines **20a** and **20b** were prepared by reacting *N*-alkyl-phenothiazines (alkyl = methyl and ethyl) with $[PdCl_2(cod)]$ (cod = 1,5-cyclooctadiene) in a 2:1 molar ratio. Complex **28b** has already been reported in the literature [19] but, to our best knowledge, its solid state structure was not confirmed. On treating two *N*-alkyl-phenotiazines (alkyl = methyl or ethyl) with $[PdCl_2(cod)]$, complexes **28a** and **28b** were obtained. The formation of the two complexes was demonstrated by X-ray diffraction measurements, the ^{1}H and ^{13}C-NMR spectra being similar with those of the starting materials.

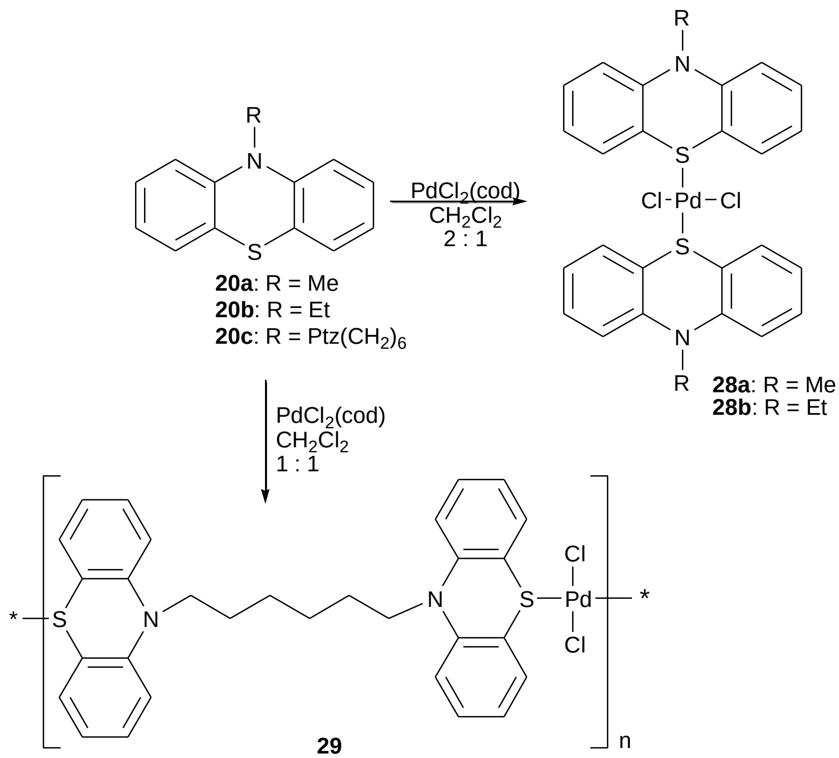

Scheme IV.1. Complexation of *N*-substituted phenothiazines towards Pd(II) (Ptz=phenothiazinyl)

Suitable crystals for X-ray diffraction measurements were grown in dichloromethane. Their solid state structures are presented in **Fig. IV.3.**

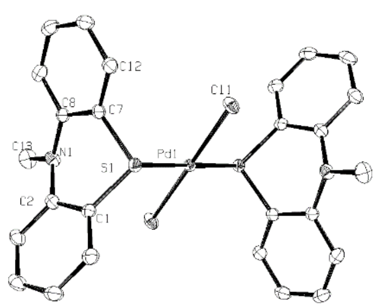

28a

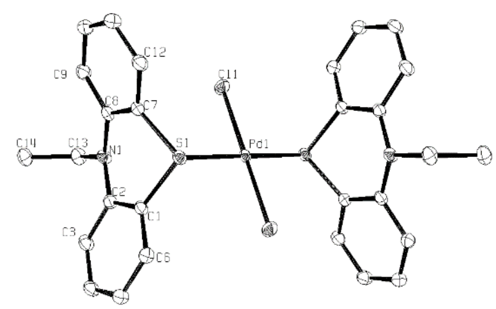

28b

Fig. IV.3. Solid state molecular structure of complexes **28a** and **28b**

Both complexes crystallize in the $P2_1/c$ space group with 2 molecules in the unit cell. The bond lengths have similar values to those observed in dichloro*bis*(phenothiazine-κS)palladium (II) [2]. The UV-vis spectra of complexes **28a** and **28b** was recorded in a dichloromethane solution.

Both compounds exhibit 3 absorption maxima — **28a**: at 254, 309 and 565 nm; **28b**: 256, 310 and 571 nm. The fluorescence spectra of compounds **28a** and **28b** was also recorded and emission at 366 and 363 nm, respectively, was observed. The quantum yields were calculated reported to naphthalene standard and it was observed that the ethyl analogue has a slightly smaller quantum yield (5.2% for **28a** and 4.1% for **28b**, compared to naphthalene). The calculated Stokes shifts are 12048 cm^{-1} for **28a** and 11514 cm^{-1} for **28b**.

Because compound **20c** has 2 sulfur atoms able to coordinate, the reaction between **20c** and [$PdCl_2$(cod)] was tried in a 1:1 molar ratio also, the proposed chemical structure is presented in **Scheme IV.1**. The ^{1}H-NMR spectrum of the palladium complex is similar to the spectrum of the starting material, but the signals are slightly shifted to lower fields (i.e., H^1 and H^9 appear in the complex at 7.00 ppm compared to 6.82 ppm in the uncoordinated phenothiazine **20c**, H^2, H^4, H^6 and H^8 appear as a multiplet at 7.40-7.44 ppm in **29** compared to 7.12-7.14 ppm in **20c**). Further investigations need to be carried out in order to undoubtedly assign a structure for compound **29**.

IV.3.2. Conclusions

N-alkyl-phenothiazines coordinate through the sulfur atom to palladium forming Pd(II) complexes when reacted in a 2:1 molar ratio with [$PdCl_2$(cod)]. Two palladium (II) complexes were prepared and characterized: the new [$PdCl_2${(10-methyl-phenothiazine)-κS}$_2$] **28a** and [$PdCl_2${(10-ethyl-phenothiazine)-κS}$_2$] **28b**, which has already been reported in the literature, but its solid state structure has not been confirmed until now. They were characterized by ^{1}H and ^{13}C-NMR spectroscopy, X-ray diffraction measurements and elemental analysis. Their UV-vis absorption and emission spectra were recorded and their quantum yields reported to naphthalene were calculated.

The reaction between 1,6-*bis*-(phenothiazin-10-yl)-hexane and [$PdCl_2$(cod)] in a 1:1 molar ratio led to the formation of complex **29**, for which a polymeric structure was proposed.

References

[1] C. Lauth, *Ber. Deut. Chem. Ges.*, *9* (**1913**) 1035.

[2] X. Zhang, D. Li, X.P. Zhou, S.W. Ng, *Acta Cryst., Section E*, *E61* (**2005**) m603.

[3] X. Zhang, W. Yu, Y. Xie, Q. Zhao, Y. Tian, *Inorg. Chem. Commun.*, *6* (**2003**) 1338.

[4] X. Zhang, Y. Xie, W. Yu, Q. Zhao, M. Jiang, Y. Tian, *Inorg. Chem.*, *42* (**2003**) 3734.

[5] J.A.H. B.J. Coe, L.J. Harrington, J.C. Jeffery, L.H. Rees, S. Houberchts, A. Persoons, *Inorg. Chem.*, *37* (**1998**) 3391.

[6] S.E. Kidd, T.W. Hambley, A. Hever, M.J. Nelson, J. Molnar, *J. Inorg. Biochem.*, *62* (**1996**) 171.

[7] R. Kroener, M.J. Heeg, E. Deutsch, *Inorg. Chem.*, *27* (**1988**) 558.

[8] B.J. Coe, J.A. Harris, L.J. Harrington, J.C. Jeffery, L.H. Rees, S. Houbrechts, A. Persoons, *Inorg. Chem.*, *37* (**1998**) 3391.

[9] J.R. Holbrook, *J. Neurochem.*, *7* (**1961**) 60.

[10] J. Byczkowski, R. Borysewicz, *Gen. Pharmacol.*, *7* (**1976**) 365.

[11] B.W.V.d. Waal, D. Feil, *Acta Cryst., Section B*, *33* (**1977**) 314.

[12] P. Marsau, B. Busetta, *Acta Cryst., Section B*, *29* (**1973**) 986.

[13] W.J. Geary, N.J. Mason, L.A. Nixon, I.W. Nowell, *J. Chem. Soc., Chem. Commun.*, (**1980**) 1064.

[14] W.J. Geary, N.J. Mason, I.W. Nowell, L.A. Nixon, *J. Chem. Soc., Dalton Trans.*, (**1982**) 1103.

[15] N.J. Mason, W.J. Geary, L.A. Nixon, I.W. Nowell, *J. Chem. Soc., Dalton Trans.*, (**1986**) 1347.

[16] S.P. Massie, *Chem. Rev.*, *54* (**1954**) 797.

[17] I.S. Pereteanu, PhD Thesis, Babes-Bolyai University, **2012**.

[18] D. Braun, R. Langendorf, *J. Praktische Chem / Chem. Zeitung*, *341* (**1999**) 128.

[19] S. Kudis, G. Helmcken, *Angew. Chem., Int. Ed.* , *37* (**1998**) 3047.

[20] S.S.C. Chu, D. van der Helm, *Acta Cryst., Section B*, *B30* (**1974**) 2489.

[21] S.S.C. Chu, D. van der Helm, *Acta Cryst., Section B*, *B31* (**1975**) 1179.

[22] D. Feil, M.H. Linck, J.J.H. McDowell, *Nature*, *207* (**1965**) 285.

[23] J.J.H. McDowell, *Acta Cryst., Section B*, *B32* (**1976**) 5.

[24] D. Drew, J.R. Doyle, *Inorg. Synth., 28* (**1990**) 346.

[25] CrysAlis Pro: Data collection and data reduction software package.

[26] SHELX: G. M. Sheldrick, *Acta Cryst.*, *A64*, (**2008**) 112.

V. Microwave-assisted synthesis and electrochemical characterization of bis-(10*H*-phenothiazin-3-yl)-methane derivatives

V.1. Introduction

The electrochemical properties of phenothiazine derivatives can be studied either dissolved in solution [7-12] or absorbed on an electrode surface [13-18]. The principal advantage of the second method is the use of small quantities of substance. In this way, the properties of the modified electrodes recommend their use as sensors/ biosensors, electrocatalysts, etc.

This chapter describes the microwave-assisted synthesis *bis*-(10*H*-phenothiazin-3-yl)-methane derivatives and the electrochemical behaviour of new electrode materials, based on these molecules by cyclic voltammetric measurements. The content of this chapter was published in *Journal of New Materials for Electrochemical Systems 12*, (**2009**) 233-238.

V.2. Original contributions

V.2.1. Microwave-assisted synthesis of *bis*-(10*H*-phenothiazin-3-yl)-methane derivatives

*Bis-(*10*H*-phenothiazin-3-yl)-methane (**31a**) was synthesized in good yields by microwave-assisted condensation of phenothiazine (**19**) with formaldehyde (37% aqueous solution) in ethanol, in the presence of strong acid catalysts (hydrochloric acid, methanesulfonic acid and trifluoroacetic acid, respectively) (**Scheme V.1.**). Best results were obtained in the presence of methanesulfonic acid. The condensation products precipitated from the reaction mixture and were easily removed by filtration. When acetic acid was employed as a solvent, higher oligomers of phenothiazine and formaldehyde were formed as major reaction products and **31a** appeared in lower amounts. The yield is slightly higher (65%) compared to 60% in the case of conventional heating.

The condensation of 10-ethyl-phenothiazine with formaldehyde (37% aqueous solution) in acetic acid solution, in the presence of methanesulfonic acid catalyst generated *bis*-(10-ethyl-3-phenothiazinyl)-methane **31b** (**Scheme V.1.**) accompanied by higher oligomers mixture.

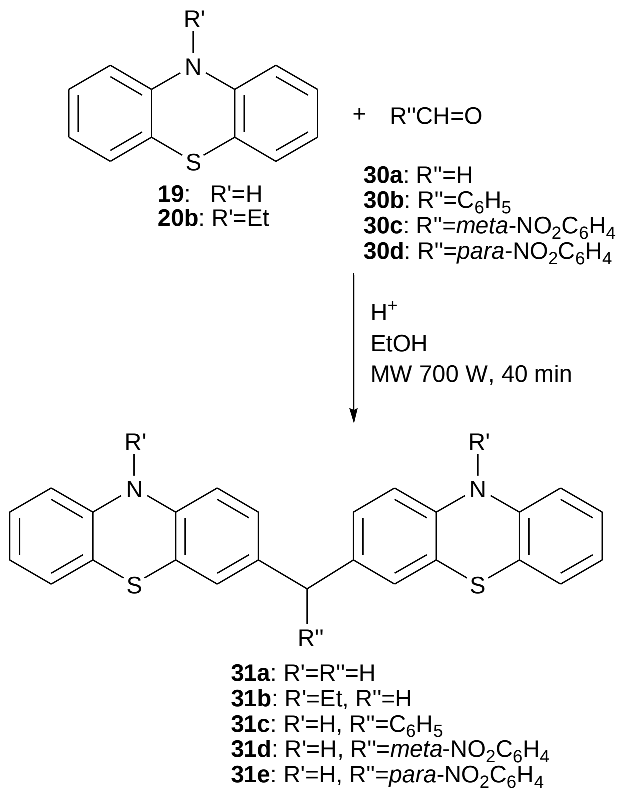

Scheme V.1. Condensation reaction of phenothiazine (**19**) and 10-ethyl-phenothiazine (**20b**) with aldehydes **30a**-**d**

Compound **31a** was characterized by NMR and FT-IR spectroscopy and EI mass spectrometry. The EI mass spectrum shows the molecular peak at *m/z* = 410; the absorption band situated at 3328 cm^{-1} in the FT-IR spectrum indicates the stretching vibration of the N-H bond. Compound **31a** can be clearly identified by the appearance of the methylene proton and carbon resonances in NMR spectra. The spectroscopic data supported the structural assignment of compound **31b**. The molecular peak in the EI mass spectrum is situated at *m/z* = 466.

The microwave-assisted condensation of phenothiazine with benzaldehyde and nitro-substituted benzaldehydes in ethanol, in the presence of acid catalyst, afforded *bis*-(10*H*-phenothiazin-3-yl)-phenyl-methane derivatives **31c**-**e** in moderate yields (**Scheme V.1.**).

Table V.1. Experimental conditions for phenothiazine and aldehyde condensation by microwave assisted synthesis (*MAOS*) *versus* conventional heating method (Δ) and electrochemical parameters of the voltammetry response for graphite electrodes modified with *bis*-(10*H*-phenothiazin-3-yl)-methane derivatives **31a**, **31c**-**e**. (Experimental conditions: scan rate 10mV s^{-1}; supporting electrolyte 0.1M phosphate buffer, pH 7).

		31a	**31b**	**31c**	**31d**	**31e**
MAOS parameters	Power (W)	700	700	700	700	700
	Temp (°C)	80	80	100	100	100
Time	Δ (h)	12	6	12	20	15
	MAOS (min)	40	20	40	40	40
Yield	Δ (%)	60	68	60	55	61
	MAOS (%)	65	60	65	58	64
E_{pa} (mV *vs* SCE)		89	-	31	9	-37
E_{pc} (mV *vs* SCE)		-59	-	-100	-94	-70
$E^{0'}$ (mV *vs* SCE)		15	-	-34.5	-42.5	-53.5
ΔE_{peak} (mV)		148	-	131	103	107
I_{pa}/I_{pc}		1.00	-	1.32	1.97	1.36
Γ (10^8 mol cm^{-2})		5.6	-	1.6	3.9	0.95

The electrochemical behaviour of *bis*-(10*H*-phenothiazin-3-yl)-methane derivatives **31a**-**e** was studied after adsorption on graphite, using cyclic voltammetry (CV) measurements. Thus, modified graphite electrodes were obtained by spreading onto the electrode surface a solution of *bis*-(phenothiazinyl)-methane derivative and leaving them to dry at room temperature. Before immersion in the test solution the modified electrodes were carefully washed with water. All the presented results are the average of at least 3 identically prepared electrodes, if not otherwise mentioned.

As expected for the redox behaviour of an *N*-unsubstituted phenothiazine moiety-containing compound [3], the formal redox potentials $E^{0'}$ (estimated as the average of cathodic and anodic peak potentials) for compound **31a** were pH-dependent (**Figure V.2.**). The protolytic mono-electronic redox equilibrium of compound **31a** is presented in **Scheme V.2**.

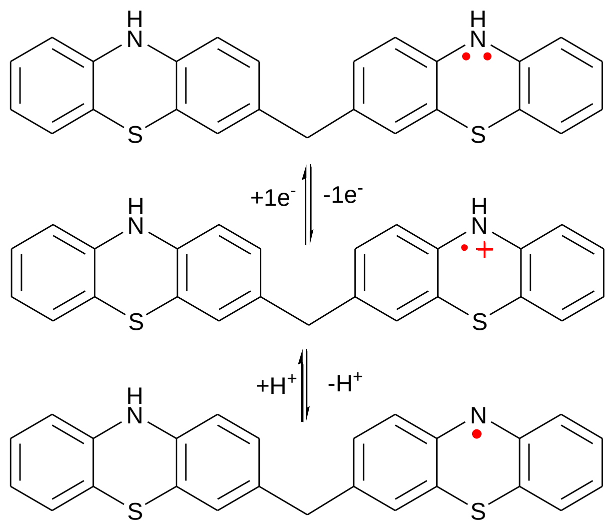

Scheme V.2. pH-dependent protolytic mono-electronic redox equilibrium of compound **31a**

V.2.2. Conclusions

Due to the efficient heating of the materials offered by the microwave power system, reduced chemical reactions times and increased reaction yields were achieved in most of the performed experiments. Compared to the conventional synthetic methods, the microwave-assisted synthesis in a pressurized system demonstrates advantages related to reaction selectivity and shorter reaction times.

Comparative study on the electrochemical behaviour of five graphite electrodes modified with *bis*-(10*H*-phenothiazine-3-yl)-methane derivatives, shows redox activity and good adsorption properties on graphite. It was established that parent compound **31a** and phenyl substituted derivatives **31c**-**e** present similar electrochemical behaviour; the electron withdrawing effect of (substituted)phenyl group supplementary attached to the methylene bridge exerts negligible influence upon the electrochemically active phenothiazine units of these *bis*-(10*H*-phenothiazin-3-yl)-methane derivatives.

References

[1] R.C. DeWald, P.O. Hong, *US Pat*., *4*, 229, (**1989**) 510.

[2] P.O. Hong, *US Pat*., *4*, 855 (**1989**) 424.

[3] S. Watarai, K. Sawada, T. Saida, *US Pat*., *4*, 229, (**1980**) 510.

[4] C.S. Kramer, T.J.J. Muller, *Eur. J. Org. Chem*., (**2003**) 3534.

[5] M. Sailer, M. Nonnenmacher, T. Oeser, T.J.J. Muller, *Eur. J. Org. Chem*., (**2006**) 423.

[6] M. Sailer, A.W. Franz, T.J.J. Muller, *Chem. Eur. J*., *14* (**2008**) 2602.

[7] G. Cauquis, A. Deronzier, J.L. Lepage, D. Serve, *Bull. Soc. Chim. France*, (**1977**) 295.

[8] G. Cauquis, A. Deronzier, J.L. Lepage, D. Serve, *Bull. Soc. Chim. France*, (**1977**) 303.

[9] M. Jitaru, C. Cristea, I.A. Silberg, *Rev. Roum. Chim*., *44* (**1999**) 865.

[10] T.Y. Wu, Y. Chen, *J. Polym. Sci., Part A: Polym. Chem*., *40* (**2002**) 4452.

[11] X. Kong, A.P. Kulkarni, S.A. Jenekhe, *Macromolecules*, *36* (**2003**) 8992.

[12] C. Buhrmester, L. Moshurchak, R.L. Wang, J.R. Dahn, *J. Electrochem. Soc*., *153* (**2006**) A288.

[13] D. Dicu, L. Muresan, I.C. Popescu, C. Cristea, I.A. Silberg, P. Brouant, *Electrochim. Acta*, *45* (**2000**) 3951.

[14] D. Gligor, L. Muresan, I.C. Popescu, I.A. Silberg, *Rev. Roum. Chim*., *47* (**2002**) 953.

[15] D. Gligor, L. Muresan, I.C. Popescu, I.A. Silberg, *Rev. Roum. Chim*., *48* (**2003**) 463.

[16] F. Fungo, S.A. Jenekhe, A.J. Bard, *Chem. Mater*., *15* (**2003**) 1264.

[17] Q. Gao, W. Wang, Y. Ma, X. Yang, *Talanta*, *62* (**2004**) 477.

[18] J.S. Abraham, R. Ramaraj, *J. Electroanal. Chem*., *561* (**2004**) 119.

[19] G. Cormos, C. Cristea, I. Filip, I.A. Silberg, *Studia UBB. Chemia*, *LI* (**2006**) 155.

[20] O. Kappe, *Angew. Chem. Int. Ed*., *43* (**2004**) 6250.

[21] P. Lindstrom, J. Tierney, B. Wathey, J. Westman, *Tetrahedron*, *57* (**2001**) 9225.

[22] M.J. Honeychurch, G.A. Rechnitz, *Electroanalysis*, *5* (**1998**) 285.

General conclusions

Eight new ferrocenyl-phosphines were prepared and characterized: monophosphines **4** and **10**, phosphonium salt **5**, phosphine oxide **6**, bisphosphines **9a** and **9b** and their palladium complexes **12a** and **12b**. Ligand **9b** and palladium complex **12b** were obtained in an enantiomerically pure form, although 4 chirality elements are present in the molecules. The coordination properties of ligand **9b** were studied towards Rh, and based on the ^{31}P-NMR spectrum a structure for complex **13** was proposed. The catalytic activity of ligand **9b** was tested in palladium catalysed C-C coupling reaction.

Two new phenothiazinyl-phosphites **16** and **18** were prepared, but purification methods failed, the compounds being characterized only by ^{31}P-NMR and mass spectrometry.

Two new phenothiazinyl-phosphine ligands were prepared and characterized (**22** and **23b**). The synthesis of **23a** and **24** has already been reported but a slightly different procedure was used; in this work they were fully characterized. The electronic properties of phenothiazinyl-phosphines **22**, **23b** and **24** were investigated by absorption/emission UV-vis spectroscopy and cyclic voltammetry. For a better understanding of their electronic properties, DFT calculations were performed on ligands **22**, **23b** and **24**.

Seven new transition metal complexes of the synthesized ligands were prepared (**25a**, **25b**, **26a**-**d** and **27b**). The formation of ligand **27a** has already been reported, but the palladium complex was not isolated. Here the solid state structure of complex **27a** is also presented.

Two new phenothiazine-palladium (II) complexes were prepared: complex **28a** and **29** and the solid state structure of already published complex **28b** was elucidated.

Five phenothiazine derivatives (**31a**-**e**) were prepared by microwave assisted synthesis. The electrochemical behaviour of these compounds was studied after adsorption on graphite, using cyclic voltammetry measurements.